Research Article

Fadi Althoey*, Osama Zaid*, Muhammad Yasir, Mohammed Awad Abuhussain, Yakubu Dodo, and Abdullah Mohamed

Experimental research on mechanically and thermally activation of nano-kaolin to improve the properties of ultra-high-performance fiber-reinforced concrete

https://doi.org/10.1515/ntrev-2024-0051 received December 8, 2023; accepted June 11, 2024

Abstract: The rising demand for ultra-high-performance concrete (UHPC) necessitates innovations in sustainable materials. This study explores the substitution of ordinary Portland cement (OPC) with thermally and mechanically activated nano-kaolin in varying proportions from 0.5 to 0.25%. A uniform quantity of double-hooked end steel fibers was added to all the mixes. Activated nano-kaolin variants showed significant enhancement in UHPC properties. Specifically, UHPC with 0.20% thermally activated kaolin (B3-TAK-20) exhibited a 21.6% increase in compressive strength and a 25.5% increase in modulus of elasticity at 90 days, with the modulus of rupture doubling compared to the reference mix. These improvements are attributed to the amorphous nature of thermally activated nano-kaolin, resulting in a denser concrete matrix and reduced porosity. Beyond the optimal 0.20% kaolin replacement, an increase to 0.25% diminished compressive strength. Durability tests showed enhanced acid resistance, with only a 6.7% mass loss for the thermally activated nano-kaolin mix and a consistent reduction in water absorption by 14.4% as kaolin proportions increased from 0.5 to 0.25%. The study also noted a

decrease in water absorption by 22.9 and 12.3% at 56 and 90 days, respectively, indicating the thermally activated nano-kaolin's enhanced performance. This research underscores the potential of activated kaolin as a viable alternative to OPC, paving the way for more sustainable UHPC production.

Keywords: recycled material, activated nano-kaolin, UHPC, acid attack, porosity, modulus of rupture

Abbreviations

CH calcium hydrate CO_2 carbon dioxide CS compressive strength **CSH** calcium silicate hydrate DHE SF double hooked end steel fibers high-range water reducer HRWR ITS indirect tensile strength MK metakaolin

MOE modulus of elasticity
MOR modulus of rupture
OPC ordinary Portland cement
PSD particle size distribution

SCMs supplementary cementitious materials

TAK thermally activated kaolin
TAM thermally activated metakaolin
UHPC ultra-high-performance concrete

UHPFRC ultra-high-performance fiber-reinforced concrete

WA water absorption

Mohammed Awad Abuhussain, Yakubu Dodo: Architectural Engineering Department, College of Engineering, Najran University, Najran, Saudi Arabia

Abdullah Mohamed: Research Centre, Future University in Egypt, New Cairo, 11835, Egypt

1 Introduction

In the last two decades, the booming construction sector has significantly driven up the demand for ordinary Portland

^{*} Corresponding author: Fadi Althoey, Department of Civil Engineering, College of Engineering, Najran University, Najran, Saudi Arabia, e-mail: fmalthoey@nu.edu.sa

^{*} Corresponding author: Osama Zaid, Department of Civil Engineering, Swedish College of Engineering and Technology, 47070, Wah Cantt, Pakistan, e-mail: Osama.zaid@scetwah.edu.pk Muhammad Yasir: Department of Civil Engineering, Swedish College of Engineering and Technology, 47070, Wah Cantt, Pakistan

cement (OPC) [1], the cornerstone of global construction due to its strength, flexibility, and affordability [2]. In recent years, concrete production, which largely depends on OPC, soared to over ten billion cubic meters annually [3], highlighting the massive scale of construction and the deep reliance on OPC for infrastructure worldwide [4]. Despite OPC's dominance, the emergence of ultra-high-performance concrete (UHPC) with its superior strength, durability, and environmental resistance has increased OPC demand even further due to UHPC's higher OPC content [5,6]. However, OPC production is energy- and resource-intensive, contributing to environmental challenges such as greenhouse gas emissions, estimated to be about 7% of global CO₂ emissions, and natural resource depletion [7]. These issues underscore the need for sustainable alternatives and eco-friendly practices in the cement industry to mitigate OPC's environmental impact [8]. There is a notable demand for cost-effective alternatives to OPC and UHPC in developing countries due to the high expenses associated with these materials [9,10]. Knowing these nations' financial constraints, there is a growing need to promote using more affordable cementation components [11]. By exploring and implementing alternative materials, such as supplementary cementitious materials (SCMs) or locally available resources, it is possible to reduce the overall cost of construction projects while maintaining satisfactory performance [12-14]. This emphasis on cost-effectiveness aims to support sustainable development and infrastructure growth in developing countries, making construction more accessible and affordable for their populations [15-17].

The research findings of Zaid et al. [18] indicate that incorporating mineral fillers into concrete mixtures positively impacts their microstructure and reduces the requirement for calcium hydroxide due to a pozzolanic reaction. This improvement is observed in various cement blends, as the modified bond composites' geometry leads to enhanced mechanical characteristics and favorable durability properties. Another study by Ahmed et al. [19] highlights that the distribution of fine pozzolan elements within the concrete paste creates multiple nucleation sites for forming hydration products, resulting in a more uniform paste. Kabeer et al. [20] suggest that the physical influence of fine grains allows for denser compaction of the mixture and minimizes the effects of barriers on the mobility of mixed particles and paste. By enhancing the bond across both stages, the microstructure and properties of the concrete are further strengthened, reinforcing the previous zone. While particle size can have both an additive and physical impact on the mixture, the pozzolanic reaction plays a more critical role. Adding pozzolan to OPC improves its mechanical longevity and strength due to interface reinforcement, resulting in a more consistent and compact paste. The term "pozzolan" originally

referred to materials like calcined earth and volcanic ash that react with lime in the presence of water and elevated temperatures. Cementitious materials, characterized by fine powder forms of aluminous and siliceous substances, react with calcium hydroxide to form mixtures when mixed with water. Althoey and Hosen [21] indicate that pozzolanic reactions alter the concrete's microstructure by consuming calcium hydroxide (C–H) and producing more calcium silicate hydrates (C–S–H), ultimately increasing its solidity. Rice husk ash, fly ash (FA), wheat straw ash [22], micro silica [23], granulated blast furnace slag [18], and metakaolin [24] are some of the OPC alternatives that have shown effectiveness as substitutes for OPC in various applications.

Kaolin is increasingly recognized for its potential to partially replace OPC in UHPC due to its reactive pozzolanic nature [25]. Its fine particles interact with calcium hydroxide during hydration, forming additional calcium silicate hydrates [26], refining UHPC's microstructure, and enhancing strength and densification while reducing permeability. Kaolin's high pozzolanic reactivity, fine size, and amorphous structure contribute to improved durability and performance of UHPC. Zaid et al. [24] showed that kaolin's inclusion in recycled aggregate concrete enhances durability through fine particles and amorphous silica. Tafraoui et al. [27] observed that kaolin addition resulted in UHPC with 250 MPa compressive and 20 MPa indirect tensile strengths, although durability improvements were not markedly different from reference samples. Due to its lower reactivity and pozzolanic activity, conventional kaolin may not significantly enhance UHPC's strength and durability [28,29]. Mechanically and thermally activating nanokaolin, however, overcomes these limitations. Mechanical activation, through grinding or milling, reduces particle size and increases surface area, increasing reactivity by facilitating more chemical reactions with calcium hydroxide during hydration [30]. This enhances UHPC's strength and densifies its matrix. Thermal activation, involving controlled heating, alters kaolin's structure, further increasing its reactivity and pozzolanic activity [27,31]. These activation processes significantly improve the pozzolanic reactivity, leading to stronger, less porous, and more durable UHPC by promoting additional calcium silicate hydrate formation [28]. The result is a denser, more robust microstructure with reduced alkali-silica reactions and better resistance to chemical attacks and environmental degradation.

1.1 Objective and significance of the present study

This study explores the impact of nano-kaolin clay, mechanically and thermally activated, as a cement substitute in

UHPC at percentages of 0.5, 0.10, 0.15, 0.20, and 0.25% by binder weight. A uniform quantity of double-hooked end steel fibers was added to all the mixes. It addresses a gap in research by assessing UHPC's engineering properties, including strength (compressive and indirect tensile strength, modulus of elasticity [MOE], and modulus of rupture [MOR]), durability (acid resistance, sorptivity, temperature endurance, and water absorption), and porosity. The focus is on how different proportions of activated nano-kaolin affect UHPC's performance. Results aim to enhance the understanding of sustainable UHPC development, providing insights into structural performance and environmental resilience and informing optimized mix designs for advanced concrete materials in construction.

2 Materials and mix design

The current research utilized and acquired a standard 53grade cement per ASTM C150 [28] from a local supplier. Its physical and chemical properties are presented in Table 1. Silica fume (SF) was also acquired from a specialist materials supplier; the SF was 99.9% pure with a surface area of 15,500 m²/kg and a specific gravity of 2.24. Kaolin in raw form was acquired from Kohat, and its physical and chemical properties are provided in Table 1. Kaolin was subjected to controlled heating for thermal activation at

Table 1: Physical and chemical properties of cement, MAK, and TAK

Property	Cement	Mechanically activated kaolin	Thermally activated kaolin
Color	Grey	Off-white	Greyish yellow
Specific gravity	3.15	2.58	2.7
Bulk density (g/cm³)	1.5	0.46	0.5
Surface area (m²/kg)	396	23,010	24,171
Chemical con	position		
SiO ₂	20.9	54.3	55.2
Al_2O_3	5.4	40.2	39.5
Fe ₂ O ₃	3.1	0.9	1.0
CaO	63.7	1.2	1.6
MgO	2.2	0.6	0.4
SO ₃	2.3	0.4	0.3
Na ₂ O	0.6	1.1	1.0
K ₂ O	1.4	1.9	2.0
TiO ₂	0.4	0.8	0.9
P_2O_5	0.3	0.5	0.6
Loss on ignition	0.7	0.1	0.5

temperatures typically 600–800°C. This process transforms the raw kaolin clay into a more reactive and amorphous material with increased pozzolanic reactivity. The calcination process removes impurities and enhances the material's pozzolanic properties, making it more suitable for cement applications. For mechanical activation, the thermally activated kaolin was then subjected to mechanical treatment, such as grinding, to further increase its surface area and reactivity. This step involves reducing the particle size and achieving a finer and more homogeneous powder, which promotes better incorporation and reactivity within the cementitious matrix. The particle size distribution (PSD) of SF, thermally and mechanically activated-kaolin is presented in Figure 1.

The design of UHPC is substantially influenced by the PSD of its constituents, which includes fine materials such as SF and activated kaolin. The PSD affects the packing density of the mix, which, in turn, is crucial for achieving the desired mechanical properties and durability of UHPC. According to the Andreasen and Andersen model [32-34], the optimal packing density is achieved when the PSD of the composite materials follows a continuous gradation curve that minimizes voids between particles. The current study presents an analysis of the PSD for SF, thermally activated kaolin, and mechanically activated kaolin, as depicted in Figure 2. The PSD data were analyzed using the Andreasen and Andersen model, which suggests that a distribution modulus (q-value) can effectively dictate the fines' ability to fill the spaces between the aggregates. For the UHPC mix, the q-value was calculated based on the PSD of the fine materials and the intended aggregate gradation. The results indicate that the fine particles of SF, TAK, and MAK exhibit a particle distribution conducive to a high packing density, as required for UHPC. By adjusting the proportions of these fine materials in the mix, the *q*-value can be manipulated to approach the ideal packing density, enhancing the concrete's strength and durability. Moreover, the PSD analysis demonstrates that the fine materials in this study significantly influence the workability and viscosity of the UHPC mix. The smaller particles of SF and activated kaolin fill the interstitial spaces between the aggregates, reducing the water demand and improving the cohesion of the mix. This results in a denser, more uniform matrix, which is essential for the high-performance characteristics of UHPC. Quartz sand was used as a fine aggregate from a special materials supplier in Peshawar. A certain proportion of polycarboxylate etherbased superplasticizer was used to maintain a uniform water-to-cement ratio (w/c).

In the present study, three batches with eleven different mixes were developed. In the first batch, no

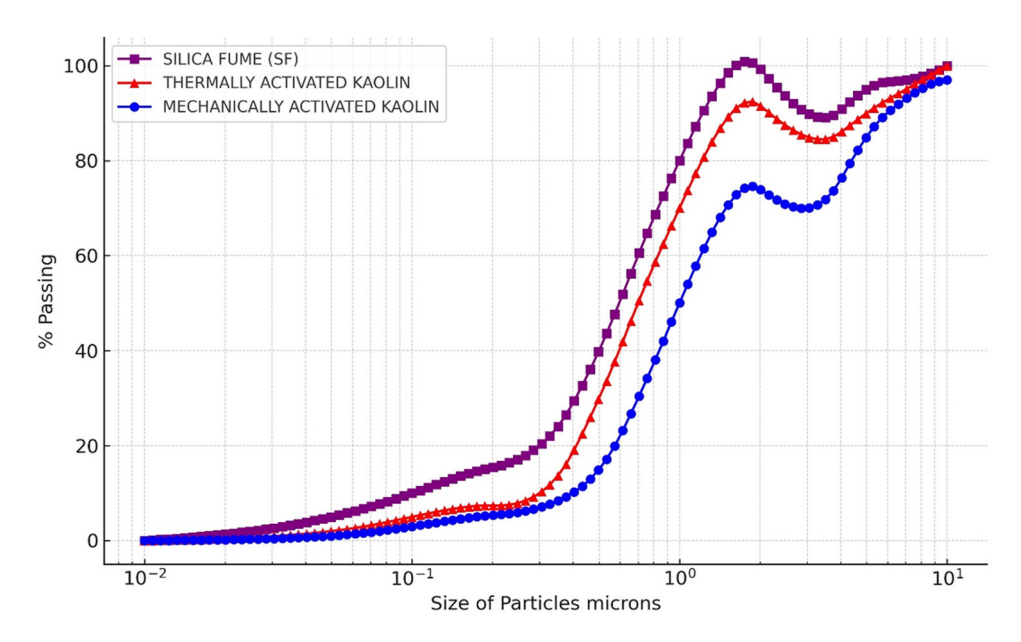


Figure 1: PSD of SF, mechanically activated kaolin, and thermally activated kaolin.

thermally and mechanically activated kaolin was added, and it was termed a reference mixture. In the second batch of mixes, different proportions (0.5, 0.10, 0.15, 0.20, and 0.25%) of mechanically activated kaolin were used in mixtures. In the third batch, 0.5, 0.10, 0.15, 0.20, and 0.25% of thermally activated kaolin were used in mixtures. The complete details of all mixes are presented in Table 2. The nomenclature of mixes was designed in such a way that the number after "B" denotes the batch number and the number after

"MAK" and "TAK" denotes the proportions of mechanically activated and thermally activated kaolin.

3 Mixing and curing procedure

For UHPC production, a high-performance mixer capable of producing a homogeneous and uniform mix is essential.

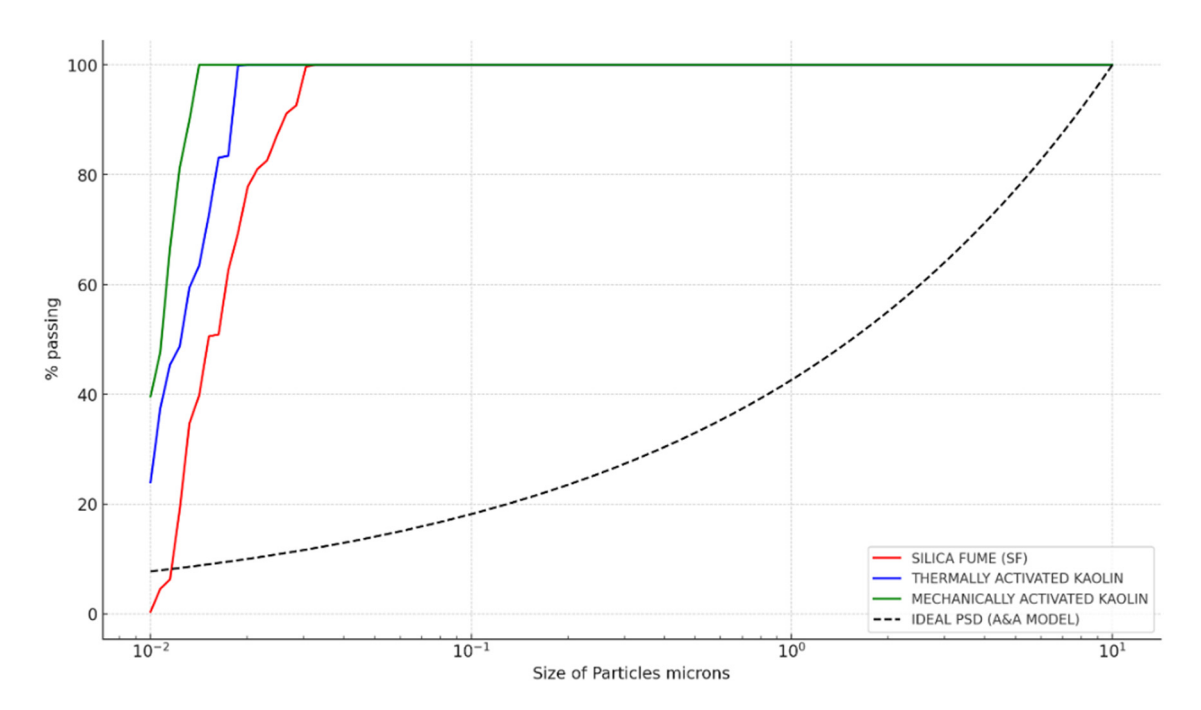


Figure 2: PSD curves for SF, thermally, and mechanically activated kaolin against the optimal Andreasen and Andersen model for UHPC.

Table 2: Complete specifics of all mixes (kg/m³)

Batch	Mix ID	OPC	SF	QS	Water	MAK	TAK	DHE SF	HRWR
Batch 1	Reference	870	130	1,215	180	0	0	25	25
Batch 2	B2-MAM-5	826.5	130	1,215	180	4.35	0	25	25
	B2-MAM-10	783	130	1,215	180	8.7	0	25	25
	B2-MAM-15	739.5	130	1,215	180	13.05	0	25	25
	B2-MAM-20	696	130	1,215	180	17.4	0	25	25
	B2-MAM-25	652.5	130	1,215	180	21.75	0	25	25
Batch 3	B3-TAM-5	826.5	130	1,215	180	0	4.35	25	25
	B3-TAM-10	783	130	1,215	180	0	8.7	25	25
	B3-TAM-15	739.5	130	1,215	180	0	13.05	25	25
	B3-TAM-20	696	130	1,215	180	0	17.4	25	25
	B3-TAM-25	652.5	130	1,215	180	0	21.75	25	25

MAK – mechanically activated nano-kaolin, TAK – thermally activated nano-kaolin, OPC – ordinary Portland cement, SF – silica fume, QS – guartz sand, DHE SF - double hooked end steel fibers, HRWR - high range water reducer.

A planetary mixer was used because it is suitable for UHPC. These mixers offer excellent mixing efficiency and can handle the high-strength and low water-to-cement ratio characteristics of UHPC. The mixing process was started by dry blending the cement, SF, quartz sand, and activated kaolin in the mixer. Dry mixing ensures an even distribution of cementitious materials and additives, minimizing the risk of clumping and improving the overall mix quality. The pre-calculated water was gradually added to the dry mix while the mixer was running. It was ensured that water was added uniformly to prevent any localized wet spots or dry pockets in the mixture. In addition to steel fibers, a polycarboxylate ether-based superplasticizer was used, which helped achieve the target workability without increasing the water content, which is vital for UHPC's high strength and durability. Allow the mixer to run appropriately to ensure thorough mixing and proper dispersion of all the components. The total mixing time was about 5 min. The mix was visually inspected to ensure no clumps or unmixed materials. As multiple batches of UHPFRC were required to be developed, consistency of the mix was maintained in the mixing process, and the same proportions of the materials and mixing time were adhered to ensure uniformity and performance across all batches. After mixing, the UHPC samples were collected for different testing, including compressive, indirect tensile strength, MOE and rupture, and durability properties.

The curing process for UHPC specimens plays a pivotal role in achieving the desired mechanical properties and durability. In the present study, a two-stage curing method was employed for the UHPC specimens to ensure optimal strength development and densification of the microstructure. After casting, the UHPC specimens were initially kept in a controlled environment at 20°C with a relative humidity of over 95% for 24 h to facilitate the hydration process. This initial period is critical for early-stage strength development and prevents premature drying that could lead to microcracking. Subsequently, the specimens underwent heat curing to expedite the pozzolanic reactions and further enhance the strength. This was done by subjecting the specimens to a temperature of 90°C for 48 h in a steam curing chamber. The elevated temperature significantly accelerates the hydration of calcium silicate phases and the reaction between SF and the calcium hydroxide released during the hydration of Portland cement, leading to the formation of additional calcium silicate hydrate gel, which is essential for the high-performance characteristics of UHPC. After the heat curing stage, the specimens were allowed to cool down to room temperature to avoid thermal shock gradually. After cooling, the specimens were de-molded and stored in a moist environment until the testing time to maintain the hydration process without any moisture loss.

This thorough curing regime was chosen based on the composition of the UHPC mix, which includes SF and activated kaolin, to achieve a dense and homogenous microstructure. It is pertinent to note that the curing method is tailored to enhance the fine materials' packing density and PSD characteristics, as depicted in Figure 2, following the Andreasen and Andersen model.

The current research employed a standardized experimental approach to investigate various mixtures and their impact on a specific characteristic. Every batch and mix underwent evaluation utilizing three specimens to certify uniformity and minimize possible errors. The results presented in the study are based on the average values derived from these specimens, offering a reliable representation of the complete performance exhibited by every individual mixture.

4 Test characterization

The flowability test was conducted on fresh UHPC mixes under ASTM C143 [35] specifications. A standard slump cone was used for this purpose, with a 200 mm internal diameter at the base, 100 mm diameter at the upper portion, and a height of 300 mm. The flow measurement was evaluated by calculating the average of the diameters of the concrete spread in a circular pattern.

The compressive and indirect tensile strength, MOE, and MOR of concrete were tested by preparing representative specimens as per applicable ASTM standards. For compressive strength testing, the cylindrical specimens (200 mm × 100 mm) were placed in a compression testing machine per ASTM C39 [36], and a gradually increasing axial load was applied until failure. The highest loading was recorded, and the compressive strength was evaluated. For indirect tensile strength, the cylindrical specimen was subjected to a diametrical load using a splitting tensile test apparatus per ASTM C496 [37], and the maximum tensile load was noted at failure. The elasticity testing method involved subjecting cylindrical specimens per ASTM C469 [38] to compression and tension loads while measuring the corresponding stress and strain at different intervals. For the MOR test, gradually increasing load was applied per ASTM C78 [39] to rectangular concrete prisms (600 mm × 200 mm × 200 mm) supported on two ends until failure. The maximum bending moment was measured and the MOR was calculated using beam dimensions and applied load.

To assess resistance to acid attack, concrete specimens (200 mm × 100 mm) were immersed per ASTM C267 [40] in 5% acidic solution (sulfuric acid H₂SO₄) by weight for 48 h, and after dipping the samples in acidic solution, the mass loss and residual compressive strength on UHPC samples cured at 90 days were evaluated. Sorptivity tests used submerged prismatic concrete discs (100 mm diameter) to determine water absorption characteristics. For exposure to elevated temperatures, concrete specimens (200 mm × 100 mm) were placed in controlled environments with increasing heat (250, 500, 750, and 1,000°C) to observe mass loss and residual compressive strength of UHPC samples cured 90 days. Water absorption tests were also performed per ASTM C1585 [41], which involved immersing concrete samples in water and calculating weight differences to gauge permeability.

Mercury intrusion porosimetry (MIP) was used for the UHPC samples' porosity test. Before testing, the specimens underwent oven-drying at 50°C until reaching a consistent mass, ensuring any residual moisture content was removed. MIP is an essential technique as it offers valuable insights into the concrete's pore size distribution, porosity, and pore

connectivity, significantly determining the material's durability and mechanical characteristics.

5 Results and discussion

5.1 Flowability test

The flowability characteristics of UHPC, including different proportions of nano-kaolin, are presented in Figure 3. The significance of Figure 3 lies in its depiction of how mechanically and thermally activated nano-kaolin impacts the concrete's fresh properties. When up to 0.20% of the cement is replaced with either MAK or TAK, there is a noticeable improvement in the UHPC's flowability. This increase in flowability can be primarily ascribed to the pozzolanic reaction initiated by kaolin. This reaction produces supplementary C-S-H gel, which diminishes the water requirement needed to achieve the desired consistency, as noted in past studies [42]. Another essential side to consider is the particulate nature of kaolin itself. These kaolin particles serve a dual role as they not only facilitate improved lubrication amongst cement grains but also enhance the overall fluid dynamics of the concrete mix. Consequently, this increases flowability, which remains prominent until the kaolin content reaches 0.20%. However, a sloping point was observed in flowability when the nano-kaolin inclusion surpassed 0.20%, specifically at 0.25%. At this stage, flowability experiences a decline. The likely motivation behind this diminished flowability is the excessive concentration of kaolin particles. Their excessive presence might prompt an accumulation, thereby upsetting the tangential motion of the cement grains, as discussed in past studies [43]. Such diminishing is counterproductive and compromises the concrete mix's flowability. The flowability of the reference mixture stands at 145 mm. However, a 0.5% cement substitution with either MAK or TAK increases flowability by around 19.3 and 29% for 173 and 187 mm, respectively. However, there is a reversal in the trend when the replacement level increases to 0.25%. Specifically, flowability records a drop of about 6.2% for B2-MAK-25 and 3.4% for B3-TAK-25 when compared with the reference mixture.

When comparing MAK with TAK in terms of their influence on flowability, it becomes evident that TAK outperforms MAK. Specifically, mixtures incorporating TAK consistently recorded the highest flow values compared to any other mixture with kaolin content. The improved performance of TAK in enhancing flowability can be traced to its production process. The thermal activation, through controlled heat treatment, enhances the pozzolanic

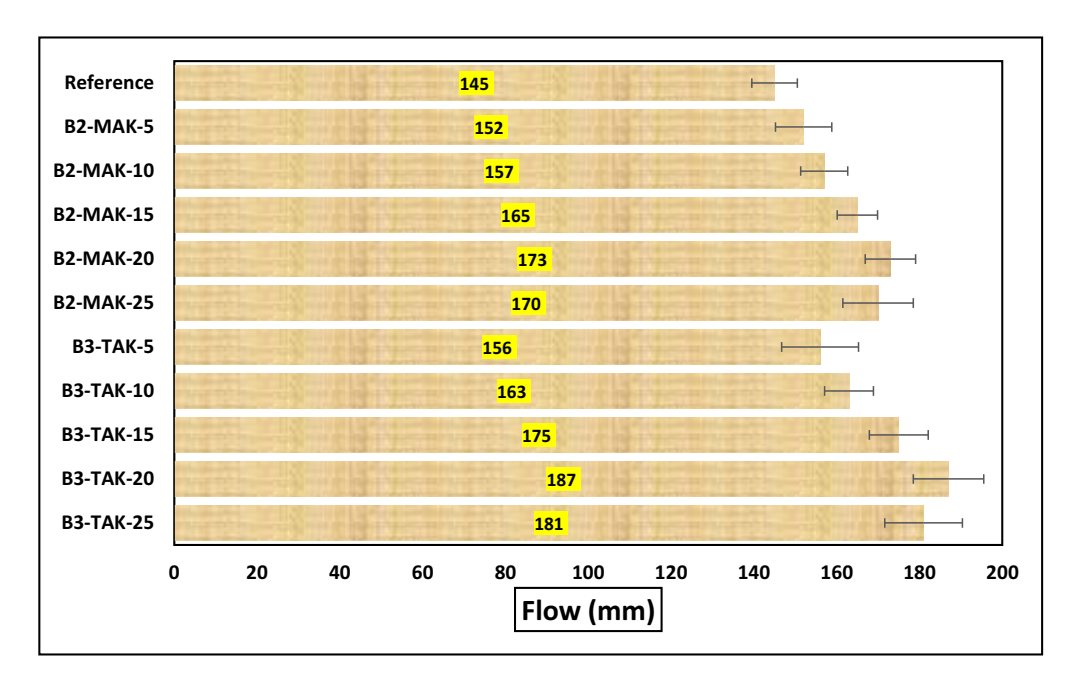


Figure 3: The flow of fresh UHPFRC.

reactivity of the kaolin. This enhanced reactivity translates into a more noticeable microstructural improvement within the UHPC matrix. Consequently, there is a notable improvement in the lubrication dynamics amongst the concrete particles, as observed in the past study [44]. This enhanced lubrication characteristic inherently gives TAKincorporated mixtures an edge in flowability over those with MAK. Furthermore, TAK showed an enhanced pozzolanic reactivity and a keen affinity to synergize with other constituents in the concrete. This proactive interaction raises a composite effect, resulting in better flowability and amplified concrete strength. Additionally, the inherent properties of TAK serve as an internal lubricant in the concrete mix, paving the way for a more optimal incorporation of all the ingredients.

Corroborating the current study findings, it is worth noting that the observed results are consistent with prior research, reinforcing the reliability of the observations. As highlighted in the study of Piasta et al. [45], there is an established precedent for the superior performance of thermally activated nano-kaolin in enhancing concrete's flowability and overall structural integrity.

5.2 Compressive strength and MOE

The test results about compressive strength and MOE at the respective intervals of 28 and 90 days are outlined in Figure 4, revealing insightful patterns and correlations. A noticeable compressive strength and MOE enhancement are apparent in samples containing 0.20% mechanically

activated nano-kaolin (B2-MAK-20) and 0.20% thermally activated nano-kaolin (B3-TAK-20). This enhancement can be unraveled by diving into kaolin's intrinsic properties and reactive capabilities as a pozzolanic material with high quantities of amorphous silica and alumina. When integrated into the concrete mix, kaolin reacts with calcium hydroxide, a byproduct of OPC hydration. The resultant calcium silicate hydrate gel, which forms, played a pivotal role as a primary contributor to the strength of cementitious materials. As such, the improved interlocking microstructure concludes in improved compressive strength. Peeling back the layers on the differential performance between mechanically activated nano-kaolin and thermally activated nano-kaolin, especially at an identical 0.20% replacement level, brings to the fore the distinct roles of reactivity and particle characteristics specific to each type. Mechanically activated nano-kaolin was subjected to a thorough grinding, increasing its surface area and instigating defects within the particles, thus rendering it highly amenable to the pozzolanic reaction. Conversely, thermally activated nanokaolin was exposed to a controlled heat treatment, which increased its reactivity by transforming a more significant proportion of the amorphous phase into the crystalline phase. As a result, thermally activated nano-kaolin catalyzes a more proficient pozzolanic reaction, leading to demonstrable gains in strength, as corroborated by Song et al. [46]. At 28 days, the compressive strength of the reference mixture stands at 122.7 MPa. Introducing 0.20% mechanically activated kaolin (B2-MAK-20) has an approximate 7% increment in strength, culminating in a measured strength of 130.4 MPa. Exploring

8 — Fadi Althoey et al. DE GRUYTER

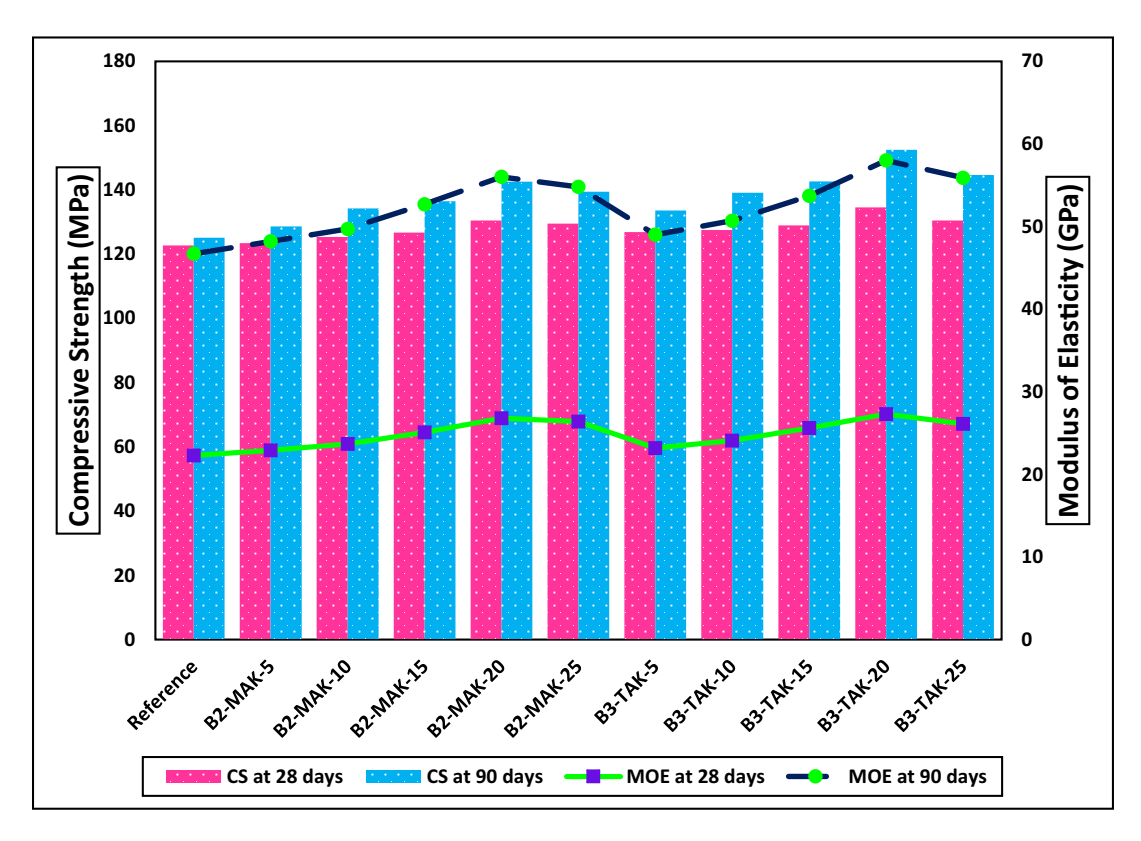


Figure 4: Compressive strength and MOE of UHPC at 28 and 90 days.

these tangible improvements in strength further illuminates the potential of kaolin as a valuable addition in modifying and enhancing the mechanical properties of UHPC, opening ways for refined material design and potential applications in more demanding structural scenarios. These enhancements and previous findings underpin the increasing interest and research in kaolin's role in optimizing concrete mixes for specialized applications, particularly where enhanced strength and durability are paramount.

Incorporating 20% thermally activated kaolin (B3-TAK-20) results in a noticeable improvement in compressive strength, evidencing an increase of approximately 9.5% over the baseline, bearing a strength value of 134.5 MPa. Also, at the 90-day mark, the reference mixture's strength rises to 125.1 MPa. The introduction of 0.20% mechanically activated nano-kaolin (B2-MAK-20) into this mix sees the strength surge by an impressive 14.3%, settling at 142.5 MPa. However, the incorporation of 0.20% thermally activated nano-kaolin (B3-TAK-20) showcases a peak of performance, registering a remarkable increase of around 21.6%, achieving a standout strength of 152.4 MPa. This observable inclination toward improved MOE in UHPC specimens, incorporating 0.20% mechanically activated nano-kaolin (B2-MAK-20) and 0.20% thermally activated nano-kaolin (B3-TAK-20), aligns intricately with the foundational principles of material science. The

augmentation in MOE can be attributed to the enhanced pozzolanic reaction and particle packing density facilitated by the nano-scale modification of kaolin through mechanical and thermal activation. These modifications significantly improve the interfacial transition zone between the cement matrix and the aggregates, leading to a denser, more homogenous microstructure. Consequently, this densification contributes to the increased mechanical properties, including the MOE, by optimizing the distribution of stresses and minimizing microcracks under applied loads. Further, the nano-scale size of the activated kaolin particles aids in filling the voids within the concrete matrix more effectively than conventional materials, thereby enhancing the overall durability and strength characteristics of the UHPC. The underlying mechanisms supporting this phenomenon are well documented within nanotechnology's application in advanced composite materials, illustrating a significant correlation between nanoparticle modification processes and the resultant mechanical properties of composite materials.

Mechanically and thermally activated nano-kaolin are intrinsically pozzolanic, with amorphous (or shapeless) alumina and silica. These components are introduced to the concrete mix to instigate a pozzolanic reaction, synergizing with the calcium hydroxide (CH) birthed during OPC hydration, as outlined in reference [47]. This catalytic

process arranges the formation of supplementary calcium silicate hydrate gel, a foundation phase with a pivotal role in increasing the strength and rigidity of the cementitious matrix, as corroborated by past studies [48]. With kaolin's incorporation, there's an increase in the C-S-H gel volume, producing a more intricate interlocking microstructure and, consequently, enhanced MOE values. At 28 days, the result reveals the reference mixture's MOE was 22.3 GPa. In 20%, mechanically activated nano-kaolin (B2-MAK-20) results in nearly 20%, achieving 26.8 GPa. Meanwhile, introducing 20% thermally activated nano-kaolin (B3-TAK-20) pushes the envelope even further, marking an ascent of around 22.3% to 27.3 GPa. At 90 days, the reference mix's elasticity modulus advanced to 24.4 GPa. The blend with 0.20% mechanically activated nano-kaolin (B2-MAK-20) reflects a growth of approximately 19.3%, reaching 29.2 GPa. Yet, it is the mixture with 20% thermally activated nano-kaolin (B3-TAK-20) that truly showcased a significant increase of around 25.5%, settling at 30.7 GPa.

An additional aspect contributing to the observed enhancement in performance metrics is the inherent particle characteristics of the nano-kaolin. The process of mechanical activation yields nano-kaolin with ultra-fine granularity. In contrast, thermal activation results in a crystalline structure of the kaolin, a transformation induced by the thermal treatment. These distinct physical states enable the nanoparticles to penetrate, fill, and strengthen

the interstitial spaces within the concrete matrix effectively, a phenomenon corroborated by previous research findings [49]. The superior packing density achieved through these nanoparticle dispersions leads to a microstructure marked by reduced porosity, minimized air entrapment, and fewer structural weaknesses. This refined micro-architecture enhances the distribution and transfer of loads across the concrete matrix, thereby increasing its stiffness. Such modifications are directly observable in the elevated MOE values, indicating a significant improvement in the material's rigidity and structural integrity. This intricate relationship between the intrinsic properties of nano-kaolin particles and the mechanical performance of the concrete underscores the importance of material selection and processing techniques in achieving desired outcomes in advanced construction materials.

5.3 Indirect tensile strength (ITS)

Figure 5 depicts the test results for ITS at 28 and 90 days. Analyzing the data reveals a substantial enhancement in ITS in the specimens containing 20% mechanically activated kaolin (B2-MAK-20) and 0.20% thermally activated nano-kaolin (B3-TAK-20). The observed increase in ITS up to 0.20% replacement level for both mechanically activated nano-kaolin (B2-MAK-20) and thermally activated kaolin

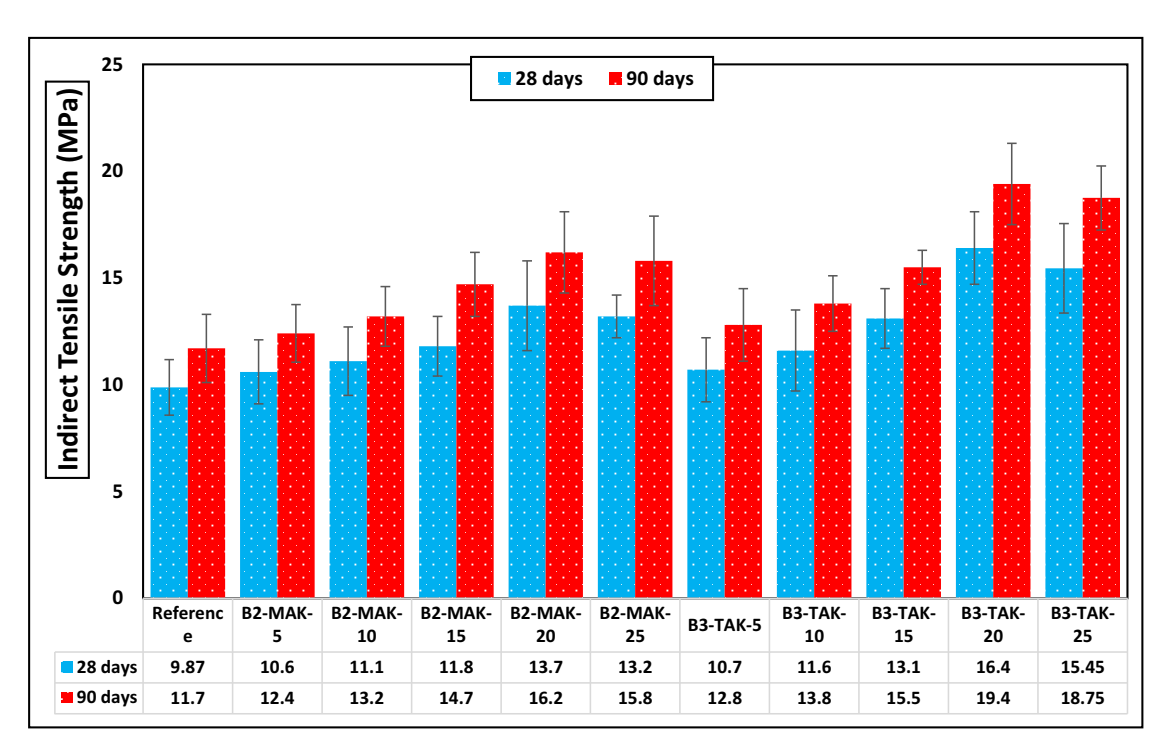


Figure 5: ITS of UHPC at 28 and 90 days.

(B3-TAK-20) can be attributed to the positive effects of the pozzolanic reaction and microstructural modifications. The increase in ITS is associated with the densification of the concrete microstructure and the reduction in porosity achieved with kaolin addition. At lower replacement levels (up to 0.20%), the fine particles of mechanically activated kaolin and the thermally activated kaolin's crystalline structure fill the voids and spaces within the matrix, reducing the overall porosity [50]. This results in improved load transfer mechanisms and enhanced tensile strength. At 28 days, the ITS of the reference mixture is 9.87 MPa. Replacing cement with 0.20% mechanically activated nano-kaolin (B2-MAM-20) increases the ITS by approximately 38% to reach 13.2 MPa, while 0.20% thermally activated nano-kaolin (B3-TAK-20) results in an increase of about 39.1% to reach 13.7 MPa. At 90 days, the ITS of the reference mixture increases to 11.7 MPa. With 20% mechanically activated nano-kaolin (B2-MAK-20), the ITS increases by approximately 35.9% to reach 15.45 MPa, while 20% thermally activated nano-kaolin (B3-TAK-20) exhibits an increase of about 38.5% to reach 16.2 MPa.

However, the reduction in ITS observed at a 0.25% replacement level for mechanically activated nano-kaolin (B2-MAK-25) and thermally activated kaolin (B3-TAK-25) can be attributed to a few factors. At higher replacement levels, excessive kaolin might lead to an overcrowded microstructure with an increased amount of unreacted kaolin particles [51]. This could cause particle agglomeration and hinder the pozzolanic reaction, leading to a less effective strengthening mechanism [31]. The ITS decreases at a 0.25% replacement level compared to the 20% level. At 28 days, the ITS for 0.25% mechanically activated nanokaolin (B2-MAK-25) is reduced by approximately 10.7% compared to B2-MAM-20, and for 0.25% thermally activated nano-kaolin (B3-TAK-25), the reduction is about 11.8% compared to B3-TAM-20. At 90 days, the decrease in ITS values for B2-MAM-25 and B3-TAM-25 compared to their 0.20% counterparts is approximately 2.8 and 4.6%, respectively. The excessive presence of kaolin might also lead to additional pores and voids due to incomplete filling, creating weak zones within the concrete matrix. These vulnerable zones can act as stress concentrators, reducing the overall ITS values.

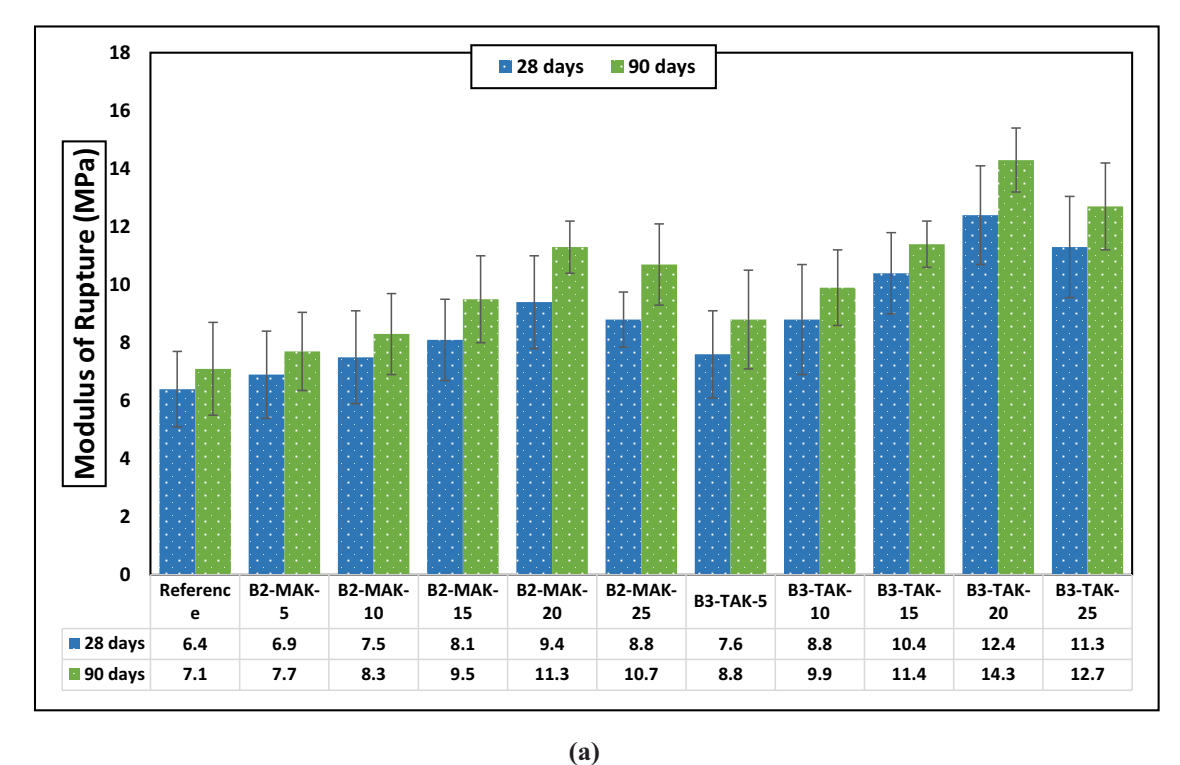
5.4 MOR

The MOR offers significant insights into the flexural strength of concrete materials, essentially determining their resistance to breakage under a bending load. Figure 6(a) explains the MOR for all samples over 28 and 90 days. When analyzing the

trends from the MOR data, an apparent pattern emerges. Incorporation of both MAK and TAK by up to 0.20% enhances the MOR. However, any further increase in their percentages seemingly inverts this trend, causing a decrement in MOR. This phenomenon underscores kaolin's pivotal role in augmenting the cementitious material's structural matrix. As a pozzolanic agent, kaolin collaborates with the calcium hydroxide developing during cement hydration, precipitating a reaction that conjures additional calcium silicate hydrate gel. This gel intensifies the adhesion and interlocking within the UHPC, a factor confirmed by another research [52]. A closer examination of the data at the 28 days reveals the MOR of the reference mixture of 6.4 MPa. Introducing a 0.20% proportion of mechanically activated kaolin (B2-MAK-20) improves the MOR to 46.9%, with values reaching 9.4 MPa.

In contrast, the same percentage of thermally activated kaolin (B3-TAK-20) takes the MOR on an even higher increase, with an almost doubling increase of around 93.8%, reaching a value of 12.4 MPa. At a 90-day interval, the MOR of the reference mixture reached 7.1 MPa. Yet, adding 0.20% mechanically activated kaolin (B2-MAK-20) propels the MOR further by a commendable 58.5%, settling at 11.3 MPa. Meanwhile, the mix modified with 0.20% thermally activated nano-kaolin (B3-TAK-20) increased by about 101.4%, with an MOR of 14.3 MPa. In addition to the pozzolanic reaction, kaolin's PSD and morphology play a crucial role in influencing MOR. Fine particles can potentially fill the voids between cement particles, creating a denser matrix less prone to cracking under bending loads. Moreover, the thermal treatment in TAK could lead to a more homogeneous PSD, which might be another reason for its superior performance compared to MAK in enhancing the MOR of the concrete.

However, at the 0.25% replacement level for mechanically activated nano-kaolin (B2-MAK-25) and thermally activated nano-kaolin (B3-TAK-25), there was a reduction in MOR compared to the 0.20% level. This reduction could be attributed to several factors. Excessive nano-kaolin leads to a congested microstructure at this higher replacement level, causing particle accumulation and potentially hindering the pozzolanic reaction. This may create weak zones or less effective bonding within the concrete matrix, decreasing the MOR values. The MOR reduces at a 0.25% replacement level compared to the 0.20%. At 28 days, the MOR for 25% mechanically activated nano-kaolin (B2-MAK-25) is reduced by approximately 6.4% compared to B2-MAK-20, and for 25% thermally activated nano-kaolin (B3-TAK-25), the reduction is about 12.1% compared to B3-TAK-20. At 90 days, the decrease in MOR values for B2-MAK-25 and B3-TAK-25 compared to their 0.20% counterparts is approximately 15.4 and 10.5%, respectively. Additionally, the microstructural



(a)

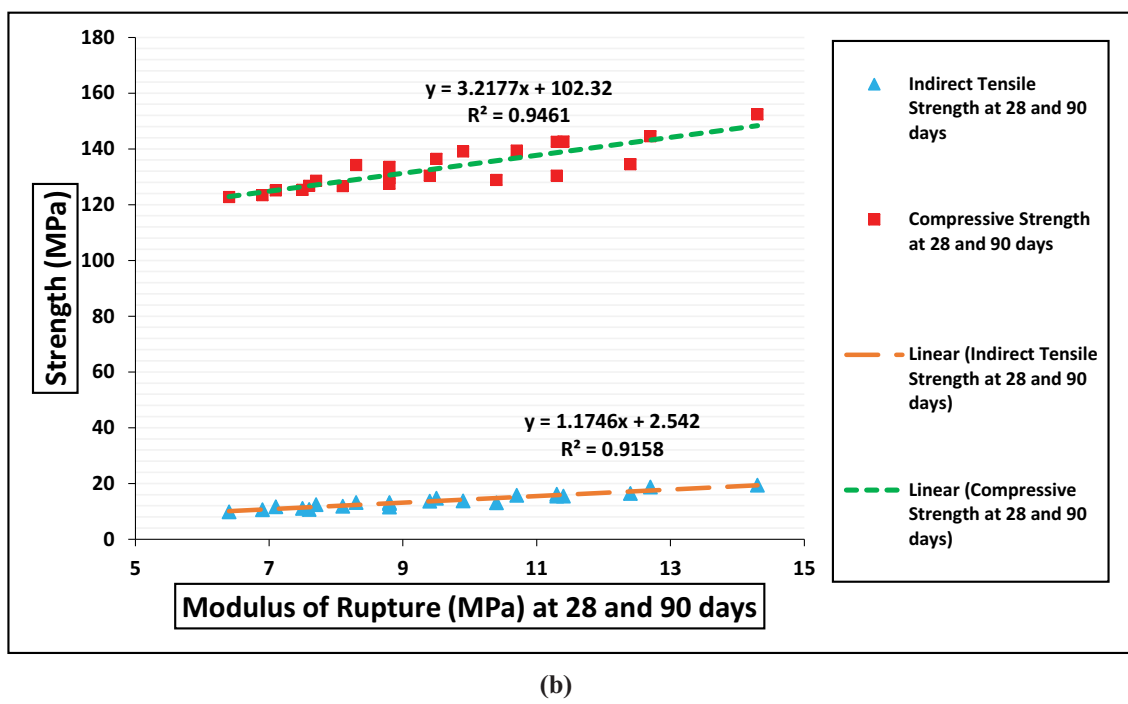


Figure 6: (a) MOR of UHPC at 28 and 90 days. (b) Statistical relationship of MOR between compressive and ITS at 28 and 90 days.

homogeneity achieved with both types of kaolin is crucial in enhancing the distribution of the pozzolanic reaction products throughout the concrete matrix. This uniformity further contributes to better load distribution and stiffness [53]. Furthermore, the synergistic relationship between the increase in MOR and the corresponding rise in MOE is unmissable. When the MOR, a measure of the concrete's resilience to bending stresses, increases, it indicates its enhanced capacity to bear loads. This capacity is shown in the improved MOE values.

The present study also employed linear regression analysis to predict the MOR (MPa) values at 28 and 90 days, utilizing the compressive and ITS values at the corresponding time points. The analysis revealed a strong linear relationship (Figure 6(b)), as evidenced by high regression coefficient values (*R*-squared) of 94.6 and 91.5% for 28 and 90 days, respectively. These high *R*-squared values indicate that approximately 94.6 and 91.5% of the variability in the MOR values can be explained by the linear relationship with the compressive strength and ITS values, respectively. Such a high level of explained variance suggests the results' robustness and accuracy, bolstering the reliability of the estimated MOR values at both 28 and 90 days.

5.5 Acid attack test

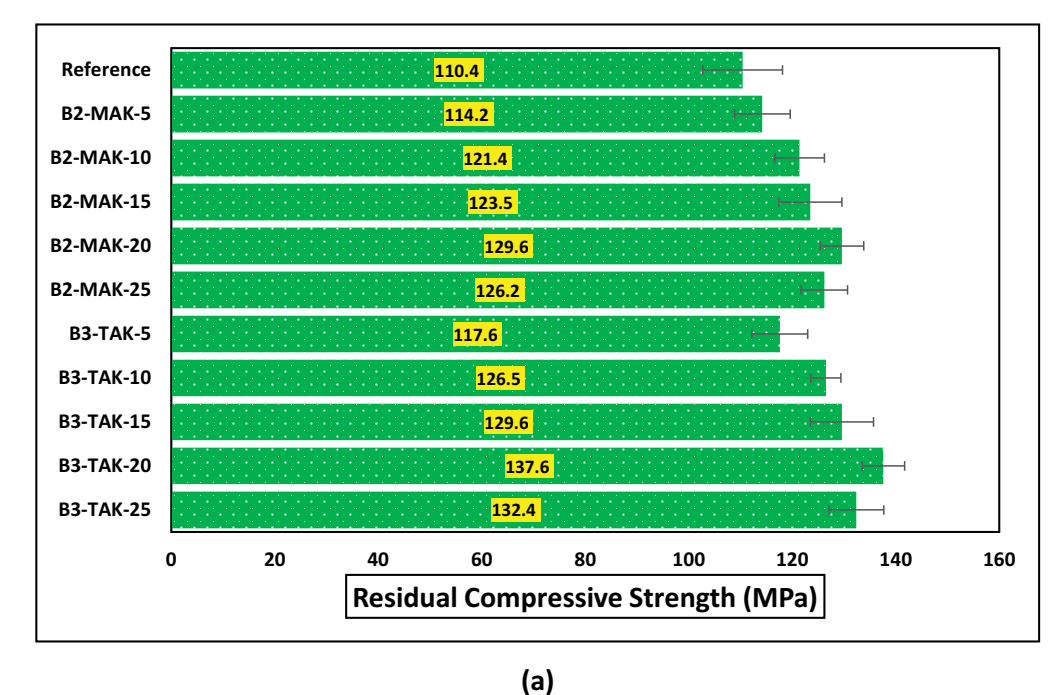
The acid attack test on all UHPC samples at 90 days is presented in Figure 7(a) and (b). For UHPC samples with up to 0.20% kaolin replacement level, both mechanical and thermal activation processes demonstrated substantial improvements in the acid resistance. Specifically, the mechanically activated nano-kaolin (B2-MAK-20) increased residual compressive strength to 129.6 MPa, surpassing the reference mixture by 17.6%. On the other hand, the thermally activated nano-kaolin (B3-TAK-20) achieved an even more impressive performance, with its compressive strength elevating by 24.4% to reach 137.6 MPa. The mass loss, a crucial indicator of material degradation under acid attack, was mitigated by including kaolin at the 0.20% replacement level. Figure 7(b) shows that mechanically activated nano-kaolin (B2-MAK-20) curtailed the mass loss by 32.3%, resulting in an 8.4% mass loss. More notably, the thermally activated nano-kaolin (B3-TAK-20) exhibited a significant reduction in mass loss of around 46.4%, recording a final loss of just 6.7%. However, an observation has occurred when the kaolin content is increased to a 25% replacement level. The performance benefits were reversed, pointing toward an optimal threshold for kaolin content in UHPC. Both types of kaolin (B2-MAK-25 and B3-TAK-25) observed a rise in mass loss and a decline in residual compressive strength. Specifically, the mechanically activated nano-kaolin (B2-MAK-25) recorded a mass loss of 9.3%, marking a 25.0% increase from its 20% counterpart. Meanwhile, the thermally activated nano-kaolin (B3-TAK-25) witnessed a 13.4% increase in mass loss, resulting in a final value of 7.6%. Regarding compressive strength, the B2-MAK-25 recorded a reduction of 2.3% compared to B2-MAK-20, whereas B3-TAK-25 observed a 3.7% reduction compared to B3-TAK-20. These findings underline the importance of optimizing the kaolin content in UHPC mixes to harness the maximum benefits of acid resistance.

The 0.20% replacement level appears optimal, with diminishing returns observed beyond this threshold.

The enhanced acid resilience of the UHPC can be drawn from incorporating kaolin into its matrix. As a recognized pozzolanic agent, kaolin instigates the formation of additional calcium silicate hydrate gel during the cement's hydration phase. This added C-S-H gel acts as a protection, develops the densification of the microstructure, and mitigates its inherent porosity. Consequently, this strong and compacted matrix emerges as a tough barrier to acid penetration [27]. Furthermore, the individual kaolin granules serve a dual function. Not only do they complement the hydration reaction, but they also settle into the interstitial spaces of the UHPC, behaving similarly to a protective layer. Their presence hinders the open infiltration of acid, shielding the concrete from the effects of corrosive entities. This protective layer appears to fade when the kaolin substitution surpasses the 0.20% mark, reaching a 0.25% replacement level, especially noticeable in mechanically activated kaolin (B2-MAK-25) and its thermally activated counterpart (B3-TAK-25). This downturn is risked to stem from an over-saturation of kaolin. At such elevated concentrations of 0.25%, the kaolin particles may clump together instead of integrating, leading to a congested and irregular microstructural scene. Such accumulations lead to weak regions undermining the concrete's acid-resisting ability [28]. Moreover, this increased (0.25%) substitution rate can skew the UHPC's intrinsic water-to-cementitious material ratio, degrading the durability, particularly when exposed to acidic attack.

5.6 Sorptivity test

The results from the sorptivity test of all UHPC samples are illustrated in Figure 8, showcasing the evolution of the sorptivity coefficient about the kaolin content. A noticeable decrease in this coefficient is apparent as the proportion of both mechanically and thermally activated kaolin increases. The underlying reason for this trend can be rooted in kaolin's instrumental role in refining the microstructure and pore topology of the concrete, thereby strengthening its resistance against water ingress. Notably, as the kaolin proportion increases from a modest 0.5% to a more substantial 0.25%, the sorptivity coefficient undergoes a consistent decline across intervals of 28, 56, and 90 days. This trajectory underscores the inference that UHPC formulations manifest an augmented imperviousness to water permeation when increased with richer kaolin concentrations. This noticeable reduction in the sorptivity coefficient is linked to kaolin's pozzolanic reactivity.



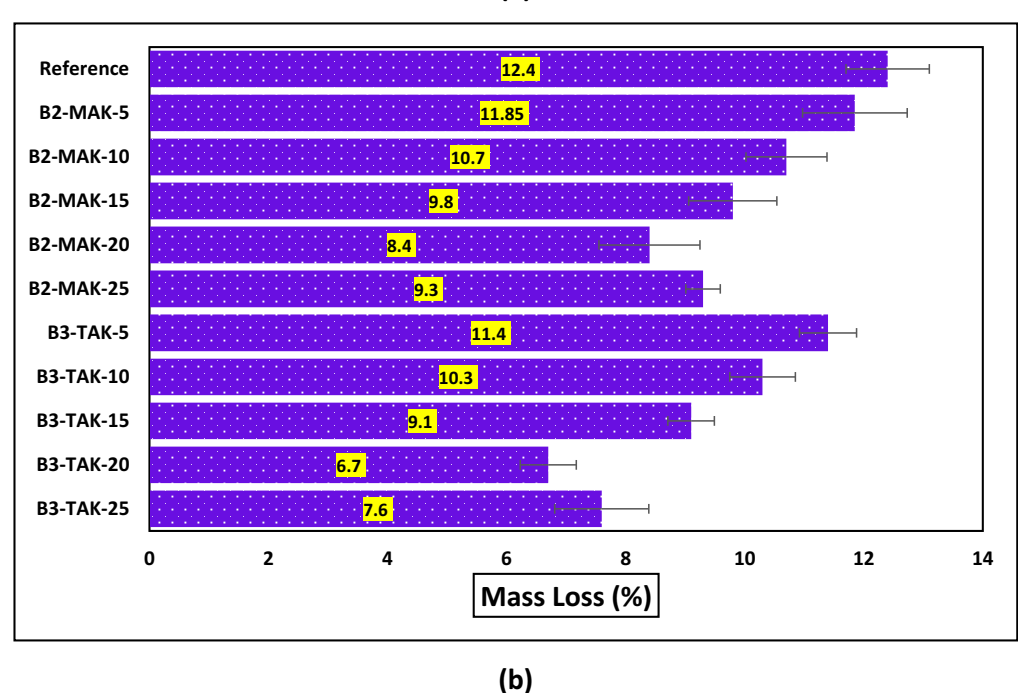


Figure 7: Acid attack test of UHPC: (a) residual compressive strength (MPa) and (b) mass loss (%).

When calcium hydroxide is a byproduct of cement hydration, kaolin undergoes a pozzolanic reaction. Given that both the mechanically and thermally activated variants of kaolin are pozzolanic, their consolidation into the UHPC leads to the creation of supplemental calcium silicate hydrate gel [54]. This gel acts as an infill, bridging voids and sealing off pores intrinsic to the concrete structure, thereby truncating the interconnected porosity network. The result is a narrowing of the pathways

that allow water to infiltrate the concrete matrix, resulting in the noted reduction in the sorptivity coefficient.

Examining the data at the 28 days, the reference mixture had a sorptivity coefficient of 0.196 mm/min^{0.5}. A 0.5% cement substitution with mechanically activated kaolin (B2-MAK-05) lowers this value by about 2.1% to 0.1912 mm/min^{0.5}. Its thermally activated counterpart, B3-TAK-05, effects a more pronounced reduction of approximately

14 — Fadi Althoey et al. DE GRUYTER

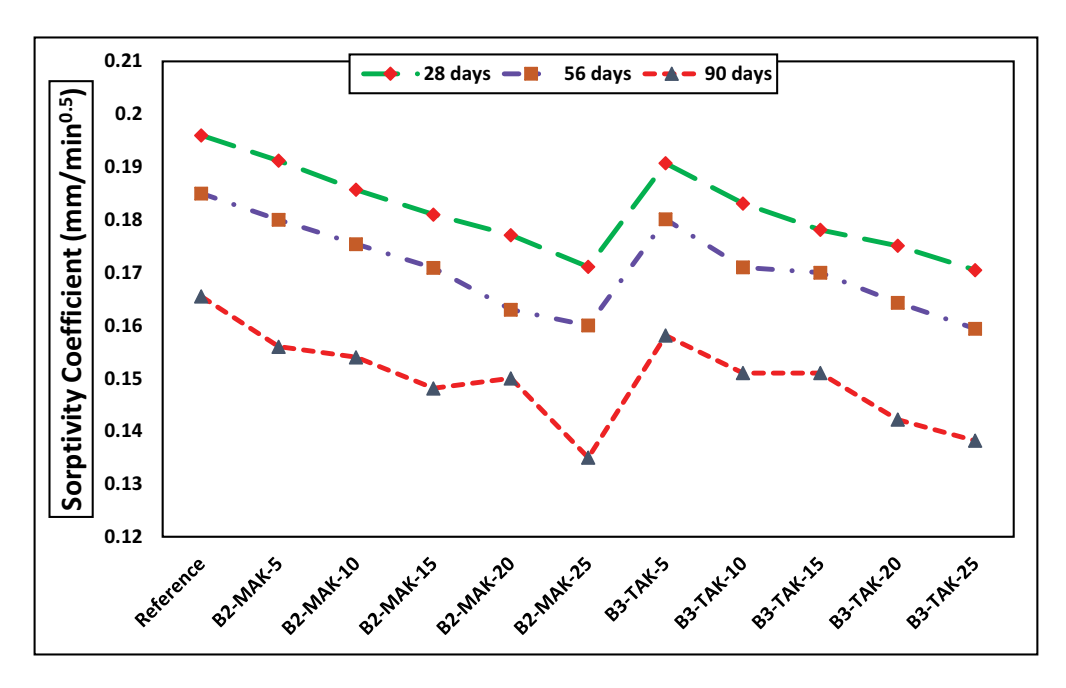


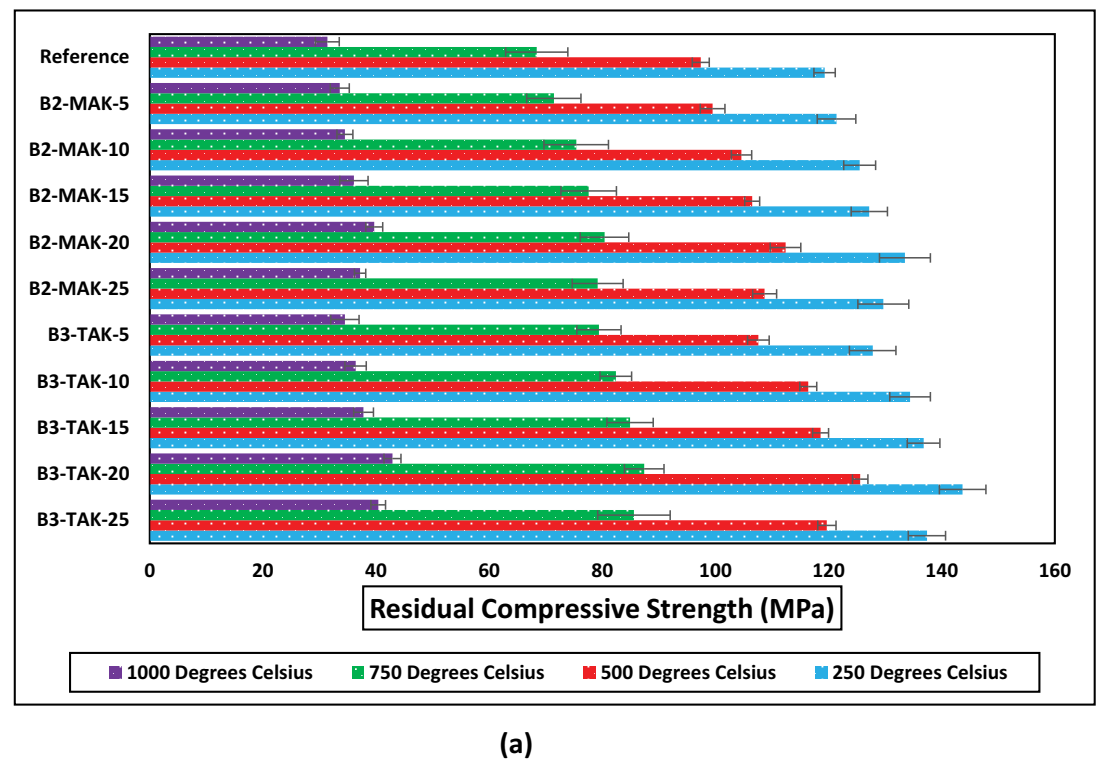
Figure 8: The sorptivity coefficient of UHPC at 28, 56, and 90 days.

5.1%, leading to a coefficient of 0.1907 mm/min^{0.5}. At 56 days, the reference blend's coefficient contracts 0.185 mm/min^{0.5}. B2-MAK-05 further reduces this by roughly 2.7% to 0.18 mm/min^{0.5}, while B3-TAK-05 observes a decrement of about 3.3%, settling at 0.1801 mm/min^{0.5}. At 90 days, the reference mix diminishes further to 0.1655 mm/min^{0.5}. Introducing 5% mechanically activated kaolin (B2-MAK-05) vields a significant drop of around 15.8% to 0.156 mm/min^{0.5}. In parallel, including 5% thermally activated kaolin (B3-TAK-05) lowers the coefficient by an estimated 14.4% to 0.1581 mm/min^{0.5}. This downward trend in the sorptivity coefficient continues until the kaolin increases to the 20% threshold for both mechanically and thermally activated forms. However, increasing this threshold and venturing to a 0.25% proportion witnesses a slight increase in the sorptivity coefficient from the 0.20% benchmark. This difference could stem from an overconcentration of kaolin, which, rather than enhancing, could disrupt the microstructural arrangement and cause an increase in the porosity and interconnected void network. Such behavior could compromise the UHPC's hydrophobic characteristics, rendering it more susceptible to water penetration [55].

5.7 Elevated temperature test

The effects of elevated temperature on all UHPC samples after a curing period of 90 days are illustrated in Figure 9(a) and (b). The changes in the residual compressive strength and mass loss, especially when subjected to a

temperature gradient spanning 250-1,000°C, support the critical role of kaolin in moderating the concrete's microstructural behavior and its inherent thermal characteristics. Notably, when the cement component in UHPC samples was substituted by up to 0.20% with both mechanically and thermally activated kaolin, a visible decline in both mass loss and the residual compressive strength was observed with increasing temperature. This trajectory emphasizes that incorporating kaolin enhances thermo-mechanical resilience in the concrete matrix [56]. The presence of kaolin resulted in the development of additional C-S-H gel over pozzolanic reactions, contributing to a more compact and denser microstructure [57]. This microstructural refinement improved thermal resistance and reduced mass loss at elevated temperatures. The sample with 0.20% thermally activated kaolin (B3-TAK-20) demonstrated the most optimal values regarding residual compressive strength and mass loss compared to the reference mixture and the samples with mechanically activated kaolin. Substituting 0.20% of cement with mechanically activated kaolin (B2-MAK-20) improved residual compressive strength compared to the reference sample at all elevated temperatures. At 250°C, the residual compressive strength is 133.5 MPa, gradually decreasing (Figure 9(a)) to 112.4, 80.4, and 39.7 MPa at 500, 750, and 1,000°C. Similarly, replacing 20% of cement with thermally activated kaolin (B3-TAK-20) resulted in an even more significant enhancement in residual compressive strength compared to the reference mixture at all elevated temperatures. At 250°C, the residual compressive strength is 143.7 MPa, decreasing to 119.7, 85.6, and 40.4 MPa at 500, 750, and 1,000°C, respectively.



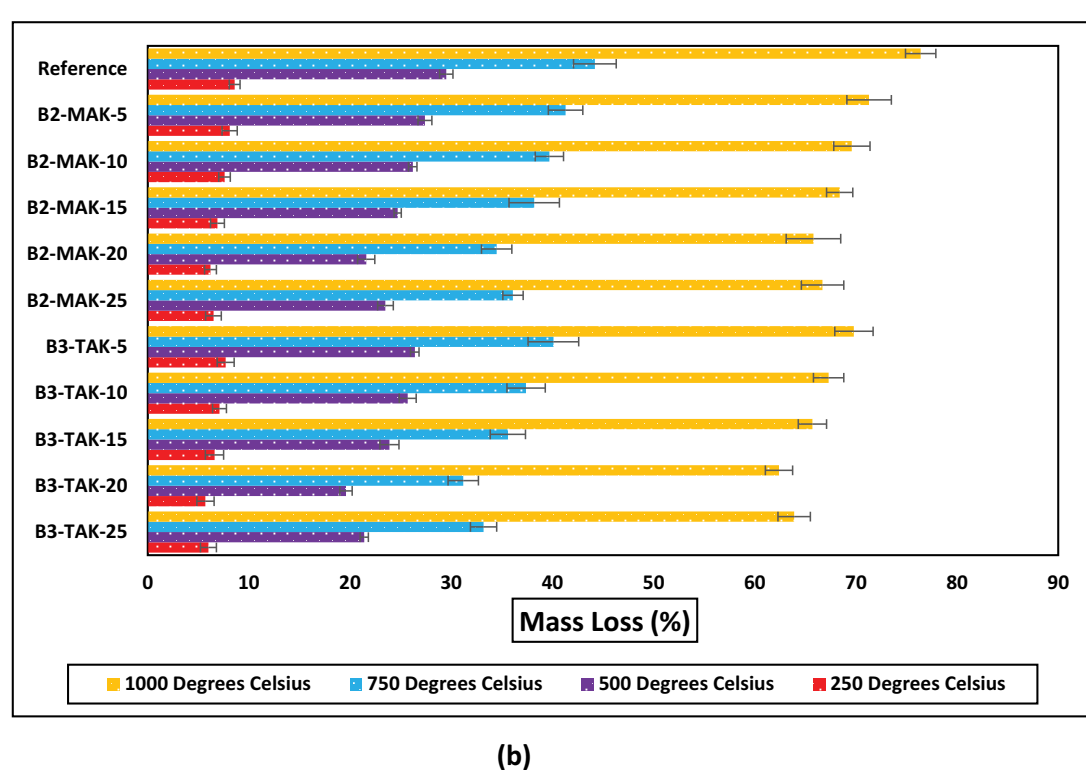


Figure 9: Elevated temperature test of UHPC: (a) residual compressive strength (MPa) and (b) mass loss (%).

The improved effectiveness observed at the 0.20% kaolin inclusion level emphasizes the benefits of the heat treatment inherent to thermally activated kaolin. This

thermal process instigates a pivotal alteration in the kaolin's intrinsic architecture, enhancing its compatibility and reactivity with the Ca(OH)₂, a by-product generated during

OPC hydration [58]. The result is tangible in the UHPC sample B3-TAK-20, characterized by a more refined microstructure and augmented thermal toughness. These features synergistically work to lower mass loss rates and improve residual compressive strength, rendering it practical to its counterpart, B2-MAK-20, and the baseline reference. However, this phenomenon hit a threshold at a kaolin inclusion of 0.25%. At this stage, both mechanically activated (B2-MAK-25) and thermally activated kaolin (B3-TAK-25) variants experience a regression in performance, particularly regarding residual compressive strength, across all evaluated high temperatures. At 250°C, B2-MAK-25 has a residual compressive strength of 129.7 MPa, reducing to 108.7, 79.2, and 37.2 MPa at 500, 750, and 1,000°C, respectively. For B3-TAK-25, the residual compressive strength at 250°C is 137.4 MPa, decreasing to 119.7 MPa, 85.6, and 40.4 MPa at 500, 750, and 1,000°C, respectively. This behavior might suggest that while introducing kaolin benefits UHPC, an excessive concentration might be counterproductive. The optimal spot appears to be around 0.20% inclusion, beyond which the benefits of kaolin diminish, and its limitations become more pronounced.

The examination of mass loss of UHPC at elevated temperatures reveals insightful findings about its behavior when subjected to heat. When analyzed at different temperature benchmarks, varying outcomes develop based on the composition of the mixture. At 250°C, the reference mixture exhibited a mass loss of 8.6%. However, the mass loss decreased substantially when 0.20% of the OPC was replaced with mechanically activated kaolin (B2-MAK-20). The reduction was 28.7%, resulting in a mass loss of 6.2%. In contrast, 20% thermally activated kaolin (B3-TAK-20) led to an even more significant reduction. The mass loss was reduced by about 33.1% to reach 5.7%. These changes are presented in Figure 9(b). When the temperature was raised to 500°C, the reference mixture demonstrated a mass loss of 29.5%. Incorporating 0.20% mechanically activated nano-kaolin (B2-MAK-20) into the mixture reduced the mass loss by approximately 26.1%, resulting in a final mass loss of 21.6%. On the other hand, using 20% thermally activated kaolin (B3-TAK-20) further reduced the mass loss by 33.4%, with the loss recorded at 19.6%. At an even higher temperature of 750°C, the reference mixture showed a mass loss of 44.2%. When 20% of cement was substituted with mechanically activated kaolin (B2-MAK-20), the mass loss decreased by about 21.9%, leading to a new figure of 34.5%. However, when 0.20% thermally activated kaolin (B3-TAK-20) was used, the reduction in mass loss was approximately 29.4%, with the mass loss registering at 31.2%. Lastly, at the extreme temperature of 1,000°C, the reference mixture had a mass loss of 76.4%. By integrating 0.20% mechanically activated kaolin (B2-MAK-20) into the

mixture, the mass loss dropped by roughly 13.1%, settling at 65.8%. Meanwhile, with 0.20% thermally activated kaolin (B3-TAK-20), the reduction in mass loss was about 18.3%, concluding at 62.4%.

However, at a 25% replacement level with both mechanically activated kaolin (B2-MAK-25) and thermally activated kaolin (B3-TAK-25), there was an increase in mass loss and a decrease in residual compressive strength at elevated temperatures compared to the 0.20% level. This trend suggested excessive kaolin content leads to a less favorable microstructure under high-temperature conditions [59]. The overcrowding of kaolin particles may create weak zones and hinder the development of an effective C-S-H gel network, resulting in reduced thermal resistance and increased mass loss [48,56,60]. These findings suggest that the addition of mechanically or thermally activated kaolin can significantly enhance the high-temperature resistance of UHPC. Among the two, thermally activated kaolin offers a more substantial reduction in mass loss across the temperature range evaluated.

5.8 Water absorption test

The water absorption test, conducted at intervals of 28, 56, and 90 days, offers intriguing insights into the behavior of UHPC samples embedded with varying proportions of mechanically and thermally activated kaolin. The graphical representation in Figure 10 emphasizes the influence of kaolin on the concrete's microstructural evolution and hydration dynamics. At 28 days, an unexpected difference was recorded across all UHPC specimens, delineating a discernible uptick in water absorption rates when juxtaposed against the reference mix. This phenomenon seemingly contradicts the anticipated performance metrics, where enhanced material processing techniques and the incorporation of nanomaterials aim to reduce porosity and water permeability. The elevation in water absorption suggests an intricate interplay between the microstructural characteristics of the UHPC formulations and their hydrodynamic behavior. Factors such as the distribution and size of pores, the efficiency of particle packing, and the presence of micro-cracks or unreacted pockets within the matrix could significantly influence water ingress. Moreover, the specific ratios of nano-kaolin can alter the hydration kinetics and the development of the cementitious matrix, potentially leading to a more porous structure. Additionally, the increase in water absorption could indicate a higher degree of interconnected porosity within the UHPC matrix, which, while detrimental to the material's resistance to water penetration, does not necessarily undermine its mechanical properties. This nuanced understanding underscores the complexity of optimizing UHPC formulations for mechanical performance and durability against environmental ingress, highlighting the need for a balanced approach in material design and engineering. This phenomenon can be traced back to the initial pozzolanic reactions between the kaolin and the calcium hydroxide formed during the cement's hydration phase [61]. Kaolin's introduction fosters the beginning of supplementary reaction by-products, notably the calcium silicate hydrate gel. This gel plays a pivotal role in refining the concrete's microstructure. Nonetheless, at this developing stage of 28 days, the concrete's microstructural maturation is incomplete, leaving open pores and voids. This partly developed microstructure results in an enhanced tendency for water absorption compared to the reference mix.

DE GRUYTER

As the curing extends to 56 and 90 days, a pronounced decline in water absorption is evident. This diminishing trend is supported by the sustained pozzolanic activity between the kaolin and calcium hydroxide [62]. With the C–S–H gel's mass and the microstructure's compaction, open porosities are progressively sealed off, regulating the paths for water ingress. Thus, by 90 days, the UHPC specimens' water absorption tendency has been significantly reduced compared to their 28-day state. At 28 days, the water absorption for the reference mixture was 10.7%. When 5% OPC was replaced with 5% MAK and TAK, water absorption increased by approximately 5.6%, reaching 11.3%.

The 0.5% thermally activated kaolin (B3-TAK-05) increased by about 12.6% to reach 12.03%. At 56 days, the water absorption for the reference mixture was 9.9%. With 0.5% mechanically activated nano-kaolin (B2-MAK-05), the water absorption decreased by approximately 8.2% to reach 9.07%, while for 0.5% thermally activated nano-kaolin (B3-TAK-05), this reduction was about 8.4% to reach 8.82%. At 90 days, the water absorption for the reference mixture was 8.68%. Substituting 0.5% of OPC with mechanically activated nano-kaolin (B2-MAK-05) decreased water absorption by approximately 1.5%, reaching 7.63%. The decrease of 5% in thermally activated nano-kaolin (B3-TAK-05) was about 1.2–7.63%.

At the 28-day interval, when 0.25% of cement was replaced by mechanically activated nano-kaolin (B2-MAK-25) and thermally activated nano-kaolin (B3-TAK-25), there was a noticeable increase in water absorption by approximately 17.8 and 19.3%, respectively. This initial increase can be attributed to the preliminary pozzolanic reactions of the kaolin variants. However, as the curing process advanced to 56 days, a prominent reversal in trend was observed. Water absorption for B2-MAK-25 decreased significantly by roughly 20.6% relative to the control mix. Similarly, for B3-TAK-25, the reduction was even more pronounced at approximately 22.9%. Continuing on this path, by the 90-day curing, B2-MAK-25 and B3-TAK-25 observed a decrease in water absorption by around 11.1 and 12.3%, respectively, when compared against the reference mixture. These results showed that the thermally activated kaolin consistently outperformed its mechanically

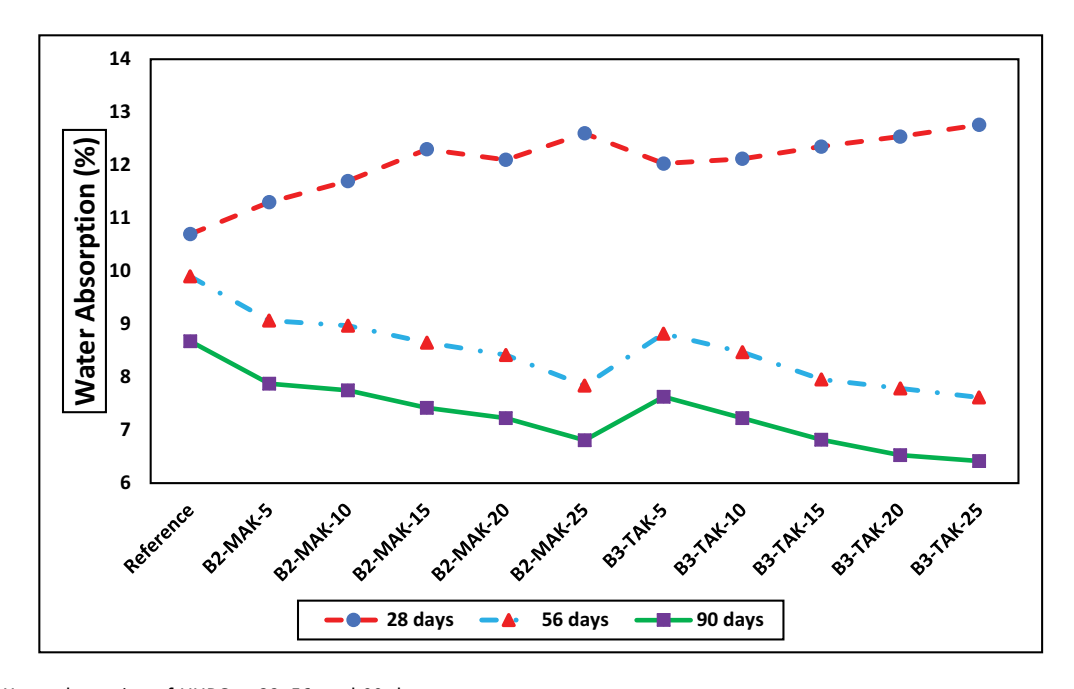


Figure 10: Water absorption of UHPC at 28, 56, and 90 days.

activated counterpart regarding water absorption during the 56- and 90-day intervals. This superiority of thermally activated nano-kaolin can be linked to its structural modifications, a consequence of the heat treatment process. This thermal activation emphasized its pozzolanic responsiveness, thereby allowing it to play a pivotal role in refining the microstructure of the concrete [63]. As a direct fallout, the concrete exhibited diminished porosity, resulting in lower water absorption values during the curing process's latter stages (56 and 90 days). However, at 28 days, thermally activated kaolin showed slightly higher water absorption than mechanically activated nano-kaolin. This could be due to the initial delay in the pozzolanic activity of thermally activated nano-kaolin during the early curing stages. As the kaolin particles require sufficient time to react with CH and form the C-S-H gel, a slight increase in water absorption is observed at this early age compared to the mechanically activated kaolin samples.

5.9 Porosity test

Figure 11 provides insight into the porosity characteristics of UHPC samples, emphasizing the impact of using mechanically and thermally activated kaolin as a cement substitute. The derived data from the graph reveal captivating insights into the interaction between pore size and porosity, essentially showcasing how the material's internal structure influences its porosity properties. The porosity test result for UHPC

shows three curve lines representing the porosity (%) at different pore diameters (nm) for three different mixtures: the reference mixture, B3-TAK-20 (sample with 0.20% thermally activated nano-kaolin), and B2-MAK-20 (sample with 0.20% mechanically activated nano-kaolin). The dashed line, representing the reference UHPC sample, exhibits the highest porosity across most pore diameters. This indicates a relatively more porous structure in comparison to the other samples. The dotted line, representing the UHPC sample with 0.20% mechanically activated kaolin (B2-MAK-20) as a partial substitute for OPC, demonstrates a noticeable reduction in porosity, especially in the smaller pore diameter range. This suggests that mechanically activated nano-kaolin has a role in refining the pore structure, leading to lower porosity. Most prominently, the solid line representing the UHPC sample with 0.20% thermally activated nano-kaolin (B3-TAK-20) showcases the lowest porosity across almost all pore diameters.

Initially, all three curve lines start at 4 nm (24%) for the reference mixture, 4 nm (11%) for B3-TAK-20, and 4 nm (14.5%) for B2-MAK-20. This indicates that all three mixtures have some porosity at this pore diameter. However, an observation was made when the pore diameter increased to around 30 nm. At this point, all three curve lines exhibit a sudden decrease in porosity, with the reference mixture's porosity dropping to 15%, B3-TAK-20 to 8%, and B2-MAK-20 to 11%. The reason behind this abrupt decrease in porosity can be attributed to the microstructure of the UHPC. At smaller pore sizes, the cementitious matrix and filler materials (such as kaolin) fill the void spaces effectively, resulting in higher porosity [64]. However, as the pore size increases,

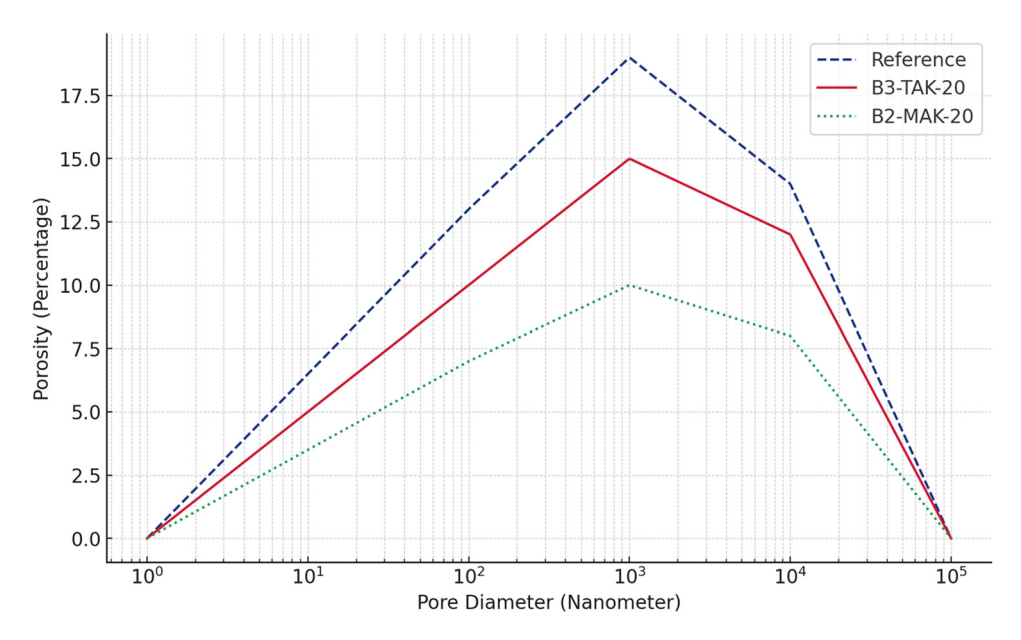


Figure 11: Porosity test of UHPC.

the microstructure of the UHPC starts to form a more compact and denser network, reducing the overall porosity. As the pore diameter continues to increase beyond 30 nm, the three curve lines show a gradual decrease in porosity. This indicates that the microstructure continues to become denser with larger pores, reducing the amount of void space within the UHPC [65]. The slight reduction in porosity observed just before the end of the curve lines at around 100,000 nm could be due to larger voids or air pockets within the concrete mix. These larger voids may be challenging to fill with the cementitious matrix, resulting in a slight increase in porosity [66].

The differences become more pronounced as the pore diameter increases towards 1,000 nm. The reference UHPC sample exhibits porosity approaching 0.20%, suggesting a more porous structure. In contrast, the B2-MAK-20 sample registers a porosity of about 15%. The most significant reduction is in the B3-TAM-20 sample, where the porosity is slightly above 10%. For larger pore diameters beyond 100,000 nm, the reference sample's porosity appears to plateau, maintaining close to 0.20%. The mechanically activated nanokaolin sample (dotted line) stabilizes around 15%. Notably, the thermally activated kaolin sample's porosity (solid line) remains the lowest, further emphasizing its effectiveness in reducing porosity, settling just above 10%. Finally, the porosity drops again when reaching 100,000 nm. This could be because huge pores might be excluded from the analysis, leading to decreased apparent porosity. The observed variations in porosity in the porosity test result for UHPC can be attributed to the microstructure of the concrete mixtures. Factors such as the size and distribution of pores, the effectiveness of filler materials like kaolin, and the overall densification of the microstructure play crucial roles in determining the porosity at different pore diameters. Understanding and optimizing the microstructure is essential in designing UHPC with desired properties such as high strength and durability. While the reference UHPC sample consistently shows the highest porosity across varying pore diameters, incorporating mechanically activated kaolin leads to up to 5% reductions. The effect of thermally activated kaolin is even more pronounced, which reduces porosity by nearly 10% compared to the reference, especially in the mid-range pore diameters.

6 Sustainability aspect of the present research

Incorporating mechanically and thermally activated nanokaolin as a partial substitute for OPC in UHPC emerges as a multifaceted strategy, fostering substantial environmental,

sustainability, and socio-economic benefits. This innovative approach directly addresses the critical environmental challenge posed by the conventional production of OPC, which is notoriously energy-intensive and a significant source of carbon dioxide emissions a predominant greenhouse gas contributing to global warming. By integrating activated kaolin into UHPC, this research contributes to a substantial reduction in the carbon footprint of construction materials, aligning with international initiatives to combat climate change and achieve ambitious carbon reduction targets. From an ecological standpoint, substituting OPC with activated kaolin mitigates the environmental degradation associated with cement manufacturing and embodies the principles of a circular economy. Kaolin activation involves valorizing kaolin clay, a plentiful natural resource, through mechanical or thermal treatments, thereby converting an otherwise underutilized material into a high-value additive for UHPC [52,67]. This utilization serves dual purposes: it reduces the reliance on virgin materials. It repurposes industrial by-products, thus diverting waste from landfills and minimizing the ecological footprint associated with waste disposal and resource extraction.

The environmental advantages are complemented by notable enhancements in UHPC's technical performance. Including activated kaolin improves critical properties such as compressive strength, durability, and resistance to aggressive environments, translating into longer lifespan and reducing maintenance demands for constructed facilities [68,69]. These improvements extend the infrastructure's service life, thereby offering economic advantages through lowered lifecycle costs and reducing the material and energy consumption associated with construction and maintenance activities. Consequently, this contributes to resource conservation and diminishes the environmental impact related to the construction sector [44,64,70]. On the socio-economic front, adopting activated kaolin in UHPC paves the way for economic development and job creation. The growing demand for sustainable construction materials necessitates advanced kaolin processing and UHPC manufacturing skills, fostering employment opportunities and stimulating local economies. Moreover, deploying sustainable construction practices enhances companies' market competitiveness by appealing to environmentally conscious stakeholders, potentially attracting investments and fostering innovation in green building technologies.

Activating kaolin into UHPC presents a complete approach to sustainable construction, marrying environmental stewardship with technological innovation and socio-economic growth. This aligns with broader sustainability goals, offering a pragmatic pathway towards more resilient, efficient, and environmentally friendly construction practices.

7 Recommendation for further studies

Based on the results and findings of the present study, several areas for further research and investigation can be recommended to deepen our understanding of the potential and applicability of activated kaolin in UHPC. Some key recommendations for future studies include the following:

- Long-term durability studies: While the current study
 provided valuable insights into the short-term durability
 of UHPC with activated kaolin, further research should
 focus on long-term durability assessments. Conducting
 accelerated aging tests and exposure to harsh environmental conditions can help assess the performance of
 activated kaolin-based UHPC over the extended service
 life, ensuring its reliability and sustainability over time.
- Incorporation of SCMs: Investigate using activated nanokaolin with other SCMs, such as SF, FA, or slag. Assessing the synergistic effects of multiple SCMs on UHPC properties can lead to even more enhanced performance and a better understanding of their potential for sustainable UHPC formulations.
- **Optimization of activation techniques:** Further explore and optimize kaolin's mechanical and thermal activation processes. Investigate alternative activation methods and varying treatment parameters to enhance kaolin's reactivity and pozzolanic properties, leading to more efficient utilization and improved UHPC performance.
- Life cycle assessment studies: Conduct life cycle assessments to comprehensively evaluate the environmental impacts of activated nano-kaolin-based UHPC compared to conventional OPC-based concrete. A thorough LCA can quantify the potential reduction in greenhouse gas emissions and resource consumption throughout the entire life cycle of the concrete, providing a holistic perspective on its sustainability.

By addressing these research areas, future research works can further enhance the comprehension and utilization of activated nano-kaolin in UHPC, ultimately advancing the development of sustainable and eco-friendly construction materials with improved performance and durability.

8 Conclusions

The present study focused on developing sustainable UHPC by incorporating different proportions of mechanically

and thermally activated nano-kaolin as a partial cement substitute. Various engineering properties of UHPC were assessed, and the following conclusions are drawn from this research:

- Replacing 5% of cement with mechanically and thermally activated nano-kaolin increases flowability by 19.3 and 29%, respectively. However, at a 0.25% replacement level, flowability decreases by approximately 6.2% (B2-MAK-25) and 3.4% (B3-TAK-25) compared to the reference mixture.
- The highest improvement in compressive strength (21.6%) and MOE (22.3%) at 90 days was observed in mixture B3-TAK-20. This can be attributed to the thermally activated nano-kaolin's crystalline structure, which fills voids in concrete more effectively, increasing packing density and reducing microstructure porosity.
- At 0.25% mechanically and thermally activated nanokaolin, a 10.7 and 11.8% reduction were observed in UHPC samples from 20% kaolin cured at 28 days despite their continuous enhancement at early proportions of kaolin.
- Replacing 0.20% of cement with MAK increased the MOR by approximately 46.9% to 9.4 MPa, while thermally activated nano-kaolin increased it by about 93.8% to 12.4 MPa. After 90 days, the reference mixture's MOR increased to 7.1 MPa. Using 20% MAK led to a 58.5% MOR increase, and 0.20% TAK resulted in a 101.4% increase.
- With 0.20%, mechanically activated nano-kaolin significantly lowered mass loss by 32.3–8.4%, while 0.20% thermally activated kaolin exhibited an even more substantial reduction of about 46.4–6.7%.
- As the proportion of nano-kaolin increased from 0.5 to 0.25%, a consistent decrease in the sorptivity coefficient was observed at 28, 56, and 90 days. With 0.5% mechanically activated nano-kaolin, the sorptivity coefficient decreases by approximately 15.8% to reach 0.156 mm/min^{0.5}. Similarly, for 0.5% thermally activated nano-kaolin, the decrease is about 14.4% to reach 0.1581 mm/min^{0.5}.
- The 0.20% kaolin with thermally activated nano-kaolin improves microstructure, thermal resistance, and strength. At 25% replacement, B2-MAK-25 and B3-TAK-25 show weakened strength at higher temperatures. At 250°C, the reference UHPC had 8.6% mass loss. With 0.20% (B2-MAK-20), it decreased by 28.7%, and 20% B3-TAK-20 by 33.1%. At 500°C, the reference had 29.5% mass loss. B2-MAK-20 was reduced by 26.1%, and B3-TAK-20 by 33.4%. At 750°C, the reference had 44.2% mass loss.
- At 28 days, 25% of B2-MAK-25 and B3-TAK-25 increased water absorption by 17.8 and 19.3%, respectively. At 56 days, it decreased by 20.6% for B2-MAK-25 and 22.9% for

- B3-TAK-25. At 90 days, B2-MAK-25 and B3-TAK-25 reduced water absorption by 11.1 and 12.3%, respectively.
- The porosity test for UHPC reveals curve lines for three mixtures: reference, B3-TAK-20, and B2-MAK-20. Smaller pore sizes have higher porosity due to effective filling, while larger pores result in a denser microstructure, reducing overall porosity. The variations in porosity are attributed to the concrete mixtures' microstructure.

Acknowledgments: The authors are thankful to the Deanship of Graduate Studies and Scientific Research at Nairan University for funding this work under the Easy Funding Program grant code (NU/EFP/SERC/13/54-2).

Funding information: The authors are thankful to the Deanship of Graduate Studies and Scientific Research at Najran University for funding this work under the Easy Funding Program grant code (NU/EFP/SERC/13/54-2).

Author contributions: All authors have accepted responsibility for the entire content of this manuscript and approved its submission.

Conflict of interest: The authors state no conflict of interest.

Data availability statement: The datasets generated and/ or analyzed during the current study are available from the corresponding author on reasonable request.

References

- Gartner E. Industrially interesting approaches to "low-CO2" cements. Cem Concr Res. 2004;34:1489-98. doi: 10.1016/j. cemconres.2004.01.021.
- Althoey F, Zaid O, de-Prado-Gil J, Palencia C, Ali E, Hakeem I, et al. Impact of sulfate activation of rice husk ash on the performance of high strength steel fiber reinforced recycled aggregate concrete. J Build Eng. 2022;54:104610. doi: 10.1016/j.jobe.2022.104610.
- Zaid O, Alsharari F, Althoey F, Elhag AB, Hadidi HM, Abuhussain MA. Assessing the performance of palm oil fuel ash and Lytag on the development of ultra-high-performance self-compacting lightweight concrete with waste tire steel fibers. J Build Eng. 2023;76:107112. doi: 10.1016/j.jobe.2023.107112.
- Mishra O, Singh SP. An overview of microstructural and material properties of ultra-high-performance concrete. J Sustain Cem Mater. 2019;8:97-143. doi: 10.1080/21650373.2018.1564398.
- Althoey F, Zaid O, Alsulamy S, Martínez-García R, de Prado Gil J, Arbili MM. Determining engineering properties of ultra-high-performance fiber-reinforced geopolymer concrete modified with different waste materials. PLoS One. 2023;18:1-32. doi: 10.1371/ journal.pone.0285692.

- Althoey F, Zaid O, Alsulamy S, Martínez-García R, de Prado-Gil J, Arbili MM. Experimental study on the properties of ultra-highstrength geopolymer concrete with polypropylene fibers and nano-silica. PLoS One. 2023;18:1-31. doi: 10.1371/journal.pone. 0282435.
- Turner LK, Collins FG. Carbon dioxide equivalent (CO2-e) emissions: A comparison between geopolymer and OPC cement concrete. Constr Build Mater. 2013;43:125-30. doi: 10.1016/j.conbuildmat. 2013.01.023.
- [8] Zhang J, Zhao Y. The mechanical properties and microstructure of ultra-high-performance concrete containing various supplementary cementitious materials. J Sustain Cem Mater. 2017;6:254-66. doi: 10.1080/21650373.2016.1262798.
- [9] Althoey F, Zaid O, Martínez-García R, de Prado-Gil J, Ahmed M, Yosri AM. Ultra-high-performance fiber-reinforced sustainable concrete modified with silica fume and wheat straw ash. | Mater Res Technol. 2023;24:6118–39. doi: 10.1016/j.jmrt.2023.04.179.
- [10] Zaid O, Zamir Hashmi SR, El Ouni MH, Martínez-García R, de Prado-Gil J, Yousef SEAS. Experimental and analytical study of ultra-highperformance fiber-reinforced concrete modified with egg shell powder and nano-silica. J Mater Res Technol. 2023;24:7162-88. doi: 10.1016/j.jmrt.2023.04.240.
- Rong Z, Wang Y, Jiao M. Optimization design and microstructure [11] analysis of ultra-high performance cement-based composites. J Sustain Cem Mater. 2023;0:1-11. doi: 10.1080/21650373.2023.
- [12] Guo Z, Jiang T, Zhang J, Kong X, Chen C, Lehman DE. Mechanical and durability properties of sustainable self-compacting concrete with recycled concrete aggregate and fly ash, slag and silica fume. Constr Build Mater. 2020;231:117115. doi: 10.1016/j.conbuildmat. 2019.117115.
- Randl N, Steiner T, Ofner S, Baumgartner E, Mészöly T. Development of UHPC mixtures from an ecological point of view. Constr Build Mater. 2014;67:373-8. doi: 10.1016/j.conbuildmat.2013. 12.102.
- [14] Li M, Zhu X, Mukherjee A, Huang M, Achal V. Biomineralization in metakaolin modified cement mortar to improve its strength with lowered cement content. J Hazard Mater. 2017;329:178-84. doi: 10. 1016/j.jhazmat.2017.01.035.
- [15] Gou H, Sofi M, Özyurt N, Zhou Z, Zhu H, Mendis P. Effect of presaturated lightweight sand on material properties of eco-friendly lightweight cementitious composites. J Sustain Cem Mater. 2023;12:561-79. doi: 10.1080/21650373.2022.2095677.
- [16] Yu Liu RJ, Yan P. Improving environmental efficiency of ultra-highperformance concrete (UHPC) through appropriate application of ultrafine quartz powder. J Sustain Cem Mater. 2023;12:941-50. doi: 10.1080/21650373.2022.2139779.
- Alghamdi H, Shoukry H, Abadel AA, Khawaji M. Performance assessment of limestone calcined clay cement (LC3)-Based lightweight green mortars incorporating recycled waste aggregate. J Mater Res Technol. 2023;23:2065-74. doi: 10.1016/j.jmrt.2023. 01.133.
- Zaid O, Mukhtar FM, M-García R, El Sherbiny MG, Mohamed AM. [18] Characteristics of high-performance steel fiber reinforced recycled aggregate concrete utilizing mineral filler. Case Stud Constr Mater. 2022;16:e00939. doi: 10.1016/j.cscm.2022.e00939.
- Ahmad J, Zaid O, Siddique MS, Aslam F, Alabduljabbar H, Khedher KM. Mechanical and durability characteristics of sustainable coconut fibers reinforced concrete with incorporation of marble powder. Mater Res Express. 2021;8:075505.

- [20] Kabeer KISA, Vyas, AK. Utilization of marble powder as fine aggregate in mortar mixes. Constr Build Mater. 2018;165:321-32.
- [21] Althoey F, Hosen A. Physical and mechanical characteristics of sustainable concrete comprising industrial waste materials as a replacement of conventional aggregate. Sustainability. 2021;13:1-12. doi: 10.3390/su13084306.
- [22] Zaid O. Martínez-García R. Aslam F. Influence of wheat straw ash as partial substitute of cement on properties of high-strength concrete incorporating graphene oxide. J Mater Civ Eng. 2022;34(11):04022295. doi: 10.1061/(ASCE)MT.1943-5533.0004415.
- [23] Zaid O, Ahmad J, Siddique MS, Aslam F, Alabduljabbar H, Khedher KM. A step towards sustainable glass fiber reinforced concrete utilizing silica fume and waste coconut shell aggregate. Sci Ren 2021:11:1-14
- [24] Zaid O, Martínez-García R, Abadel AA, Fraile-Fernández FJ, Alshaikh IMH, Palencia-Coto C. To determine the performance of metakaolin-based fiber-reinforced geopolymer concrete with recycled aggregates. Arch Civ Mech Eng. 2022;22:114. doi: 10.1007/ s43452-022-00436-2.
- [25] Albidah A, Alsaif A, Abadel A, Abbas H, Al-Salloum Y. Role of recycled vehicle tires quantity and size on the properties of metakaolin-based geopolymer rubberized concrete. J Mater Res Technol. 2022;18:2593-2607. doi: 10.1016/j.jmrt.2022.03.103.
- [26] Kannan V, Ganesan K. Chloride and chemical resistance of self compacting concrete containing rice husk ash and metakaolin. Constr Build Mater. 2014;51:225-34.
- [27] Tafraoui A, Escadeillas G, Vidal T. Durability of the Ultra High Performances Concrete containing metakaolin. Constr Build Mater. 2016;112:980-7. doi: 10.1016/j.conbuildmat.2016.02.169.
- [28] Abdellatief M, AL-Tam SM, Elemam WE, Alanazi H, Elgendy GM, Tahwia AM. Development of ultra-high-performance concrete with low environmental impact integrated with metakaolin and industrial wastes. Case Stud Constr Mater. 2023;18:e01724. doi: 10.1016/j. cscm.2022.e01724.
- [29] El-Mir A, Nehme SG, Assaad JJ. Effect of binder content and sand type on mechanical characteristics of ultra-high performance concrete. Arab J Sci Eng. 2022;47:13021-34. doi: 10.1007/s13369-022-06733-5.
- [30] Nguyen Phuong Amanjean E, Vidal T. Low cost ultra-high performance fiber reinforced concrete (uhpfrc) with flash metakaolin. Key Eng Mater. 2014;629-630:55-63. doi: 10.4028/www.scientific.net/ KEM.629-630.55.
- [31] Tafraoui A, Escadeillas G, Lebaili S, Vidal T. Metakaolin in the formulation of UHPC. Constr Build Mater. 2009;23:669-74. doi: 10. 1016/j.conbuildmat.2008.02.018.
- [32] Yu R, Song Q, Wang X, Zhang Z, Shui Z, Brouwers HJH. Sustainable development of ultra-high performance fibre reinforced concrete (UHPFRC): Towards to an optimized concrete matrix and efficient fibre application. J Clean Prod. 2017;162:220-33. doi: 10.1016/j. jclepro.2017.06.017.
- [33] Yu R, Spiesz P, Brouwers HJH. Mix design and properties assessment of Ultra-High Performance Fibre Reinforced Concrete (UHPFRC). Cem Concr Res. 2014;56:29-39. doi: 10.1016/j. cemconres.2013.11.002.
- [34] Indhumathi S, Praveen Kumar S, Pichumani M. Reconnoitring principles and practice of modified andreasen and andersen particle packing theory to augment engineered cementitious composite. Constr Build Mater. 2022;353:129106. doi: 10.1016/j. conbuildmat.2022.129106.

- [35] ASTM C143/C143M-15a. Standard test method for slump of hydraulic-cement concrete. ASTM International; 2015.
- [36] ASTM C39/C39M-17. A-C. Standard test method for compressive strength of cylindrical concrete specimens. West Conshohocken: ASTM International; 2017.
- [37] ASTM C496 / C496M-17. Standard test method for splitting tensile strength of cylindrical concrete specimens. West Conshohocken, PA: ASTM International: 2017.
- [38] ASTM C469 -14. Standard test method for static modulus of elasticity and poisson's ratio of concrete in compression. West Conshohocken, PA: ASTM International; 2014.
- [39] ASTM C. Standard test method for flexural strength of concrete (using simple beam with third-point loading). American Society for Testing and Materials: 2010. p. 12959-9428.
- [40] ASTM C 267. Standard test methods for chemical resistance of concrete, grouts, and monolithic surfacing and polymer concretes.
- [41] ASTM C1585. Standard test method for measurement of rate of absorption of water by Hydraulic-cement concretes. West Conshohocken: American Society for Testing and Materials International; 2013.
- [42] Saleh S, Li Y-L, Hamed E, Mahmood AH, Zhao XL. Workability, strength, and shrinkage of ultra-high-performance seawater, sea sand concrete with different OPC replacement ratios. J Sustain Cem Mater. 2023;12:271-91. doi: 10.1080/21650373.2022.2050831.
- [43] Shui Z, Xuan D, Chen W, Yu R, Zhang R. Cementitious characteristics of hydrated cement paste subjected to various dehydration temperatures. Constr Build Mater. 2009;23:531-7. doi: 10.1016/j. conbuildmat.2007.10.016.
- [44] Luan C, Zhang Q, Wu Z, Han Z, Zhou Z, Du P, et al. Uncovering the role of hydrophobic silica fume (HPS) in rheology, hydration, and microstructure of ultra-high-performance concrete (UHPC). J Sustain Cem Mater. 2023;12(11):1399-413. doi: 10.1080/21650373. 2023.2222398.
- [45] Piasta I, Sawicz Z, Rudzinski L, Changes in the structure of hardened cement paste due to high temperature. Matér Constr. 1984;17:291-6. doi: 10.1007/BF02479085.
- [46] Song Q, Yu R, Wang X, Rao S, Shui Z. A novel self-compacting ultrahigh performance fibre reinforced concrete (SCUHPFRC) derived from compounded high-active powders. Constr Build Mater. 2018;158:883-93. doi: 10.1016/j.conbuildmat.2017.10.059.
- [47] Taborda-Barraza M, Padilha F, Silvestro L, Azevedo AR, Gleize PJ. Evaluation of CNTs and SiC whiskers effect on the rheology and mechanical performance of metakaolin-based geopolymers. Materials (Basel). 2022;15(17):6099. doi: 10.3390/ma15176099.
- [48] Zhang B, Yu J, Chen W, Liu H. Failure evolution and fiber toughing mechanism of ultra-high performance concrete under uniaxial compression. J Sustain Cem Mater. 2023;12:441-59. doi: 10.1080/ 21650373.2022.2076264.
- [49] Kan L, Lv J, Duan B, Wu M. Self-healing of engineered geopolymer composites prepared by fly ash and metakaolin. Cem Concr Res. 2019;125:105895. doi: 10.1016/j.cemconres.2019.105895.
- [50] Ramyar K. Comparison of fly ash, silica fume and metakaolin from mechanical properties and durability performance of mortar mixtures view point. Constr Build Mater. 2014;70:17.
- [51] Mardani-Aghabaglou A, Sezer GI, Ramyar K. Comparison of fly ash, silica fume and metakaolin from mechanical properties and durability performance of mortar mixtures view point. Constr Build Mater. 2014;70:17-25.
- [52] Abdellatief M, Abd Elrahman M, Elgendy G, Bassioni G, Tahwia AM. Response surface methodology-based modelling and optimization

- of sustainable UHPC containing ultrafine fly ash and metakaolin. Constr Build Mater. 2023;388:131696. doi: 10.1016/j.conbuildmat. 2023.131696.
- [53] da Luz G, Gleize PJP, Batiston ER, Pelisser F. Effect of pristine and functionalized carbon nanotubes on microstructural, rheological, and mechanical behaviors of metakaolin-based geopolymer. Cem Concr Compos. 2019;104:103332. doi: 10.1016/j.cemconcomp.2019. 05.015.
- [54] Abbas S, Soliman AM, Nehdi ML. Exploring mechanical and durability properties of ultra-high performance concrete incorporating various steel fiber lengths and dosages. Constr Build Mater. 2015;75:429–41. doi: 10.1016/j.conbuildmat.2014.11.017.
- [55] Shi C, Wu Z, Xiao J, Wang D, Huang Z, Fang Z. A review on ultra high performance concrete: Part I. Raw materials and mixture design. Constr Build Mater. 2015;101:741–51. doi: 10.1016/j.conbuildmat. 2015.10.088.
- [56] Izadifard RA, Moghadam MA, Sepahi MM. Influence of metakaolin as a partial replacement of cement on characteristics of concrete exposed to high temperatures. J Sustain Cem Mater. 2021;10:336–52. doi: 10.1080/21650373.2021.1877206.
- [57] Li Y, Pimienta P, Pinoteau N, Tan KH. Effect of aggregate size and inclusion of polypropylene and steel fibers on explosive spalling and pore pressure in ultra-high-performance concrete (UHPC) at elevated temperature. Cem Concr Compos. 2019;99:62–71. doi: 10. 1016/j.cemconcomp.2019.02.016.
- [58] Zhang T, Zhang M, Shen Y, Zhu H, Yan Z. Mitigating the damage of ultra-high performance concrete at elevated temperatures using synergistic flame-retardant polymer fibres. Cem Concr Res. 2022;158:106835. doi: 10.1016/j.cemconres.2022.106835.
- [59] Liang X, Wu C, Yang Y, Li Z. Experimental study on ultra-high performance concrete with high fire resistance under simultaneous effect of elevated temperature and impact loading. Cem Concr Compos. 2019;98:29–38. doi: 10.1016/j.cemconcomp.2019. 01.017.
- [60] Luan C, Zhang Q, Wu Z, Han Z, Zhou Z, Du P. Uncovering the role of hydrophobic silica fume (HPS) in rheology, hydration, and microstructure of ultra-high-performance concrete (UHPC). J Sustain Cem Mater. 2023;12:1399–413. doi: 10.1080/21650373.2023. 2222398.

- [61] Dong E, Yu R, Fan D, Chen Z, Ma X. Absorption-desorption process of internal curing water in ultra-high performance concrete (UHPC) incorporating pumice: From relaxation theory to dynamic migration model. Cem Concr Compos. 2022;133:104659. doi: 10.1016/j. cemconcomp.2022.104659.
- [62] Azreen NM, Rashid RS, Amran YM, Voo YL, Haniza M, Hairie M. Simulation of ultra-high-performance concrete mixed with hematite and barite aggregates using Monte Carlo for dry cask storage. Constr Build Mater. 2020;263:120161. doi: 10.1016/j.conbuildmat. 2020.120161.
- [63] Pyo S, Kim H-K. Fresh and hardened properties of ultra-high performance concrete incorporating coal bottom ash and slag powder. Constr Build Mater. 2017;131:459–66. doi: 10.1016/j. conbuildmat.2016.10.109.
- [64] Rong Z, Jiang G, Sun W. Effects of metakaolin on mechanical and microstructural properties of ultra-high performance cementbased composites. J Sustain Cem Mater. 2018;7:296–310. doi: 10. 1080/21650373.2018.1496860.
- [65] Sohail MG, Kahraman R, Al Nuaimi N, Gencturk B, Alnahhal W. Durability characteristics of high and ultra-high performance concretes. J Build Eng. 2021;33:101669. doi: 10.1016/j.jobe.2020.101669.
- [66] Wang D, Shi C, Wu Z, Xiao J, Huang Z, Fang Z. A review on ultra high performance concrete: Part II. Hydration, microstructure and properties. Constr Build Mater. 2015;96:368–77. doi: 10.1016/j. conbuildmat.2015.08.095.
- [67] Kathirvel P, Sreekumaran S. Sustainable development of ultra high performance concrete using geopolymer technology. J Build Eng. 2021;39:102267. doi: 10.1016/j.jobe.2021.102267.
- [68] Li Z. Drying shrinkage prediction of paste containing meta-kaolin and ultrafine fly ash for developing ultra-high performance concrete. Mater Today Commun. 2016;6:74–80. doi: 10.1016/j.mtcomm. 2016.01.001
- [69] Hassaan MM, Khater HM, El-Mahllawy MS, El Nagar AM. Production of geopolymer composites enhanced by nano-kaolin material. J Adv Ceram. 2015;4:245–52. doi: 10.1007/s40145-015-0156-y.
- [70] Zhidan Rong YW, Jiao M. Optimization design and microstructure analysis of ultra-high performance cement-based composites. J Sustain Cem Mater. 2023;12:1376–86. doi: 10.1080/21650373.2023. 2219263.